

**T.C.  
ERCIYES UNIVERSITY  
GRADUATE SCHOOL OF NATURAL AND APPLIED  
SCIENCE  
DEPARTMENT OF PHYSICS**

**INVESTIGATING THE MECHANICAL AND  
MICROSTRUCTURE PROPERTIES OF Al-5Zn-2.5Mg  
ALLOYS OBTAINED BY MELT -SPINNING TECHNIQUE**

**Prepared By  
Ali M. IBRAHIM**

**Supervisor  
Prof. Dr. Mustafa KESKIN**

**M. Sc. Thesis**

**December 2017**

**KAYSERİ**

**T.C.  
ERCIYES UNIVERSITY  
GRADUATE SCHOOL OF NATURAL AND APPLIED  
SCIENCE  
DEPARTMENT OF PHYSICS**

**INVESTIGATING THE MECHANICAL AND  
MICROSTRUCTURE PROPERTIES OF Al-5Zn-2.5Mg  
ALLOYS OBTAINED BY MELT -SPINNING TECHNIQUE**

**M. Sc. Thesis**

**Prepared By  
Ali M. IBRAHIM**

**Supervisor  
Prof. Dr. Mustafa KESKIN**

**Supported by the Erciyes University Research Funds, Grant No: FYL- 2017-7348.**

**December 2017**

**KAYSERİ**

### COMPLIANCE WITH SCIENTIFIC ETHICS

I hereby declare that all information in this document has been obtained and presented in accordance with academic rules and ethical conduct. I also declare that, as required by these rules and conduct, I have fully cited and referenced all material and results that are not original to this work.



Owner of Thesis

Ali Mawlood IBRAHIM

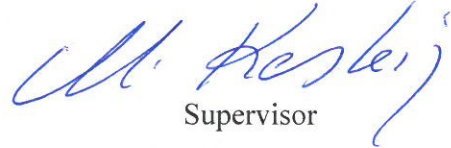
### COMPLIANCE WITH GUIDELINES

The MS thesis entitled “**INVESTIGATING THE MECHANICAL AND MICROSTRUCTURE PROPERTIES OF Al-5Zn-2.5Mg ALLOYS OBTAINED BY MELT SPINNING TECHYNIQUE**” has been prepared in accordance with Erciyes University Graduate Education and Teaching Institute Thesis Preparation and Writing Guide.



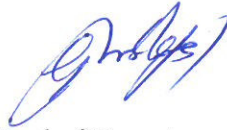
Owner of Thesis

Ali Mawlood IBRAHIM



Supervisor

Prof. Dr. Mustafa KESKIN



Head of Department

Prof. Dr. Mustafa Bergaslan

### ACCEPTANCE AND APPROVAL PAGE

This study entitled “INVESTIGATING THE MECHANICAL AND MICROSTRUCTURE PROPERTIES OF Al-5Zn-2.5Mg ALLOYS OBTAINED BY MELT SPINNING TECHYNIQUE” Prepared by Ali Mawlood IBRAHIM under the supervision of Prof. Dr. Mustafa Keskin was accepted by the jury as MSc. Thesis in physics department.

24.12/2017

### JURY:

Supervisor: Prof. Dr. Mustafa KESKIN



Juror: Prof. Dr. Mehmet GÜNDÜZ

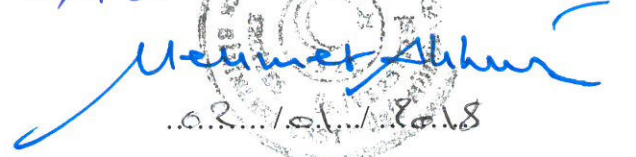


Juror: Doç. Dr. Ercan KARAKÖSE



### APPROVAL

That the acceptance of this thesis has been approved by the decision of the Institute's Board of Directors with the 02/01/2018.. date and 2018/01-57.. numbered decision.



Prof. Dr. Mehmet AKKURT

Director of the Institute

## ACKNOWLEDGEMENTS

I would like to express my special appreciation and thanks to my teacher and advisor Prof. Dr. **Mustafa KESKIN**, he has been a great mentor for me. I would like to thank him for his encouragement and for allowing me to grow as a research scientist. His advice on my thesis and academic career was priceless.

I would especially like to thank Assoc. Prof. **Ercan KARAKÖSE**, he has been there to support me in the experimental field and collecting data for my M.Sc. thesis.

A special thanks to my family Father and mother (may Allah bless their souls) words cannot express how grateful I am. My brothers and sisters, my faithful friends who were always exist to help me thank you all.

At the end I would like to express maximum appreciation to my beloved wife **Rawaa** and daughters **Maryam** and **Malak**. They were always my support in the moments when there was no one to answer my queries.

Ali M. IBRAHIM

Kayseri, December 2017

# **INVESTIGATING THE MECHANICAL AND MICROSTRUCTURE PROPERTIES OF AL-5ZN-2.5MG ALLOYS OBTAINED BY MELT -SPINNING TECHNIQUE**

**Ali M. IBRAHIM**

**Erciyes University, Graduate School of Natural and Applied Sciences**

**M.Sc. Thesis, December 2017**

**Thesis Supervisors: Prof. Dr. Mustafa KESKIN**

## **ABSTRACT**

The mechanical and microstructural properties of the conventionally solidified (CS) Al-5Zn-2.5Mg alloy were produced in a vacuum furnace by casting 99.99% pure Al, Zn and Mg, and the rapidly solidified (RS) ribbons samples for the same alloy have been obtained by the Melt-Spinning Technique (MST) with different wheel speeds of (10, 50 and 80) m/s have been investigated using the Vickers microhardness tester (VMT) with various peak loads at room temperature, also tested under a universal testing machine for the tensile tests, Scanning Electron Microscopy (SEM), X-Ray Diffraction (XRD), Differential Thermal Analysis (DTA). The tensile tests show that there are huge enhancements in the MS samples tensile stress curves than those in the CS samples. It has been found that the MS ribbon thickness has an inverse proportional to the melt-spun wheel speeds. The SEM analysis showed that the CS samples have a dendritic  $\alpha$ -Al solid solution and non-equilibrium phases. On the other hand, the melt-spun (MS) ribbons of 10, 50, and 80 m/s wheel speeds have been showed more homogeneity than that in the CS samples. The XRD patterns for the CS samples revealed two intermetallic phases ( $\text{Al}_{12}\text{Mg}_{17}$  and  $\text{MgZn}_2$ ) and the  $\alpha$ -Al phase. While no peaks corresponding to the intermetallic phases for the MS ribbons obtained by 50 and 80 m/s wheel speeds. The melting temperature for the MS ribbons of 10, 50 and 80 m/s wheel speeds were 660 °C, 660°C and 662 °C, respectively.

**Keywords:** Al-5Zn-2.5Mg alloy, Rapid solidification, Microstructure, Microhardness.

**INVESTIGATING THE MECHANICAL AND MICROSTRUCTURE  
PROPERTIES OF AL-5ZN-2.5MG ALLOYS OBTAINED BY MELT -SPINNING  
TECHNIQUE  
Ali M. IBRAHİM**

**Erciyes Üniversitesi, Fen Bilimleri Enstitüsü**

**Yüksek Lisans Tezi, Aralık 2017**

**Tez Danışmanı: Prof. Dr. Mustafa KESKİN**

**ÖZET**

Geleneksel katılaştırılmış (CS) Al-5Zn-2.5Mg alaşımının mekanik ve mikroyapısal özellikleri döküm yoluyla vakumlu bir fırında % 99.99 saf Al, Zn ve Mg üretildi ve (10, 50 ve 80) m / s 'lik farklı devir hızlarında Melt-Spinning Tekniği (MST) kullanılarak Üretilmiştir hızla katılaşmış (RS) alaşım şerit numuneleri, Vickers mikrosertlik test cihazı (VMT) kullanılarak incelenmiştir. Tarama Elektron Mikroskopisi (SEM), X-Işını Kırınımı (XRD), Diferansiyel Termal Analiz (DTA), ve ayrıca, CS ve RS numuneleri çekme testleri kullanılarak analiz edilmiştir. Gerilme testleri, MS numunelerinin çekme gerilmesi eğrilerini CS numunelerinden daha yüksek olduğunu göstermektedir. MS şerit kalınlığının, hızlı katılaştırılmış alaşımları dDK hızıyla ters bir orantıya sahip olduğu tespit edilmiştir. SEM analizi, CS numunelerinin bir dendritik  $\alpha$ -Al katı çözeltiye ile birlikte intermetalik fazlara sahip olduğunu gözlemiştir. Öte yandan, 10, 50 ve 80 m / s tekerlek hızlarındaki üretilmiş MS şeritler CS numunelerinden daha homojen mikroskopiye sahip olduğu görülmüştür. CS numuneleri için XRD modelleri, iki intermetalik faz ( $Al_{12}Mg_{17}$  ve  $MgZn_2$ ) ve  $\alpha$ -Al fazı tespit edilmiştir. 50 ve 80 m / s 'lik dönme hızlarıyla elde edilen MS şeritleri için intermetalik fazlara karşılık gelen hiçbir pik yoktu. 10, 50 ve 80 m / s dönme (dDK) hızlarındaki MS şeritlerinin erime sıcaklığı sırasıyla 660 °C, 660 °C ve 662 °C'dir.

**Anahtar kelimeler:** Al-5Zn-2.5Mg alaşım, Hızlı katılaşma, Mikroyapı, Mikrosertlik.



## CONTENTS

### INVESTIGATING THE MECHANICAL AND MICROSTRUCTURE PROPERTIES OF AL-5ZN-2.5MG ALLOYS OBTAINED BY MELT-SPINNING TECHNIQUE.

COMPLIANCE WITH SCIENTIFIC ETHICS .....	i
COMPLIANCE WITH GUIDELINES .....	ii
ACCEPTANCE AND APPROVAL PAGE .....	iii
ACKNOWLEDGEMENTS .....	iv
ÖZET .....	vi
ABSTRACT .....	v
CONTENTS .....	vii
LIST OF SYMBOLS AND ABBREVIATIONS .....	ix
LIST OF TABLES AND FIGURES .....	xi

## CHAPTER 1

1.1.INTRODUCTION.....	1
-----------------------	---

## CHAPTER 2

### GENERAL INFORMATION

2.1. ALUMINUM .....	4
2.2. ZINC .....	5
2.3. MAGNESIUM.....	6
2.4. ALLOYS.....	7
2.4.1. THE IMPORTANCE OF ALLOYS .....	7
2.4.2. THE IMPORTANCE OF THE Al-Zn-Mg ALLOYS.....	8
2.5. BACKGROUND .....	9

## CHAPTER 3

### MATERIALS AND METHODS

3.1. MATERIALS .....	17
3.1.1. MELT SPINNING TECHNIQUE.....	17
3.1.2. VICKERS MICROHARDNESS TESTER (VMT) .....	18

<b>3.1.3. UNIVERSAL TESTING MACHINES .....</b>	<b>19</b>
<b>3.1.4. SCANNING ELECTRON MICROSCOPE (SEM).....</b>	<b>20</b>
<b>3.1.5. X-Ray DIFFRACTION (XRD) .....</b>	<b>20</b>
<b>3.1.6. DIFFERENTIAL THERMAL ANALYSIS (DTA) .....</b>	<b>21</b>
<b>3.2 EXPERIMENTAL METHODS .....</b>	<b>22</b>

## **CHAPTER 4**

### **RESULTS AND DISCUSSION**

<b>4.1 THE MECHANICAL PROPERTIES.....</b>	<b>28</b>
<b>4.2. THE SEM MICROGRAPHS .....</b>	<b>32</b>
<b>4.3 THE XRD ANALYSIS.....</b>	<b>34</b>
<b>4.4 THE DTA ANALYSIS.....</b>	<b>37</b>

## **CHAPTER 5**

### **CONCLUSION**

<b>5.1 The Vickers and Tensile Stress Results .....</b>	<b>41</b>
<b>5.2 The SEM Results.....</b>	<b>41</b>
<b>5.4 The DTA Results .....</b>	<b>42</b>
<b>REFERENCES .....</b>	<b>43</b>
<b>CURRICULUM VITAE .....</b>	<b>48</b>

## LIST OF SYMBOLS AND ABBREVIATIONS

$\sigma$	Tensile stress
$\eta'$	Metastable phase
$\lambda_1$	Primary dendrite arm spacing
$\lambda_2$	secondary dendrite arm spacing
A	Total sample cross area
Al	Aluminum
Al <sub>3</sub> Zr	Zirconium aluminide
Ag	Silver
ASAX	Anomalous Small Angle X- ray scattering
APT	Atom Probe Tomography
at%	Atomic percentage
Cao	Lime
CS	Conventional Solidification
Cu	Copper
°C	Celsius degree
Cr	Chromium
DTA	Differential Thermal Analysis
Fe	Iron
G	Temperature Gradient
GP I, GP II	Guinier – preston Zones
Hv	Vickers hardness
HREM	High Resolution Electron Microscopy
K	Kelvin
KN	Kilo Newton
K/s	Kelvin per Second
K/mm	Kelvin per millimeter
M	Magnification factor
$\mu\text{v}$	Micro Volt
$\mu\text{m}$	Micro Meter
MS	Melt-Spun
m/s	Meter per second

Mm	Millimeter
Mpa	Mega Pascal
Mg	Magnesium
MgO	Magnesia
MgCl <sub>2</sub>	Magnesium Chloride
Mn	Manganese
nm	Nanometer
OM	Optical Microscopy
PFZ	Precipitate free zone
RST	Rapid Solidification Technique
Si	Silicon
SEM	Scanning Electron Microscopy
Ti	Titanium
T6	Solution heat treatment and artificially aged
T7	Solution heat treatment and stabilized (over aged)
TEM	Transmission Electron Microscopy
V	Growth rate
Wt%	Weight percentage
XRD	X-ray Diffraction
Zn	Zinc
Zr	Zirconium

## LIST OF TABLES AND FIGURES

<b>Table. 1</b>	Aluminum alloys groups.....	7
<b>Table. 2</b>	The Dependence of the microhardness ( $H_v$ ) on wheel speed of 10 and 80 m/s for the melt-spun Al-5Zn-2.5Mg ribbons and the CS samples.....	31
<b>Figure 3.1</b>	Melt spinning process [33] .....	17
<b>Figure 3.2</b>	Vickers microhardness test .....	20
<b>Figure 3.3</b>	Tensile Strain test schematic .....	21
<b>Figure 3.4</b>	SEM analysis schematic .....	22
<b>Figure 3.5</b>	XRD analysis principle .....	18
<b>Figure 3.6</b>	DTA schematic .....	19
<b>Figure 3.7</b>	The CS alloy ingot.....	22
<b>Figure 3.8</b>	Metacut-m250 device [44].....	23
<b>Figure 3.9</b>	Sectioned samples .....	23
<b>Figure 3.10</b>	Graphite crucible .....	23
<b>Figure 3.11</b>	Melt-spinning process .....	24
<b>Figure 3.12</b>	MS alloy ribbons .....	24
<b>Figure 3.13</b>	Struers Lapopress 1 device .....	24
<b>Figure 3.14</b>	Hot mounting ribbon sample .....	25
<b>Figure 3.15</b>	Hot mounting process clips.....	25
<b>Figure 3.16</b>	Struers Labopol 5 device [45].....	25
<b>Figure 3.17</b>	Diamond Suspension .....	26
<b>Figure 3.18</b>	The MS ribbons and CS samples after hot mounting and polishing .....	28
<b>Figure 4.1</b>	The variation of the Vickers microhardness values with applied test load for the CS samples .....	32
<b>Figure 4.2</b>	The variation of the Vickers microhardness values with applied test load for the MS ribbons of 10 and 80 m/s .....	30
<b>Figure 4.3</b>	Engineering stress-strain curves obtained by the tensile tests at room temperature for the CS samples. ....	32
<b>Figure 4.4</b>	Engineering stress-strain curves obtained by the tensile tests at room temperature for the MS ribbons of 10 and 80 m/s .....	34
<b>Figure 4.5</b>	The SEM images for the CS sample .....	35
<b>Figure 4.6</b>	The SEM images for the MS samples at 10 m/s. ....	36
<b>Figure 4.7</b>	The SEM images for the MS samples at 50 m/s. ....	36

<b>Figure 4.8</b>	The SEM images for the MS samples at 80 m/s. ....	37
<b>Figure 4.9</b>	The XRD patterns for the CS samples. ....	38
<b>Figure 4.10</b>	The XRD patterns for the MS samples at 10 m/s.....	39
<b>Figure 4.11</b>	The XRD patterns for the MS samples at 50 m/s.....	39
<b>Figure 4.12</b>	The XRD patterns for the MS samples at 80 m/s.....	40
<b>Figure 4.13</b>	The DTA analysis for the MS samples at 10 m/s .....	29
<b>Figure 4.14</b>	The DTA analysis for the MS samples at 50 m/s .....	29
<b>Figure 4.15</b>	The DTA analysis for the MS samples at 80 m/s .....	40
<b>Figure 4.16</b>	Variation of the Al-5Zn-2.5Mg ribbon thicknesses as a function of the wheel speeds for the MS samples.....	41

## **CHAPTER 1**

### **1.1.INTRODUCTION**

The science of materials is one of the most important sciences in the advanced industrial countries. It is a renewable science in which researches and studies are conducted to obtain new materials with special characteristics. The materials science has a quite contact with the scientific researches such as physics, chemistry, and engineering. Since the ancient times, the mankind has been interested in the development of the minerals and the creation of new strong metals for using in everyday life as well as in the battles [1]. The Minerals are very important for the development of the human civilization. At the beginning of the human evolution, the humans used natural materials such as animal skins, stones, clay, and wood. When the Copper was discovered and reinforced by mixing with other minerals (alloying), the Bronze Age appeared. The use of the iron and the steel, which are strong metals used in the wars to give excellent chances to win has appeared around 1200 BC. The next new important step was establishing the steel industry around the year 1850, which started with the manufacture of the train lines and structures with modern installation. Metal properties are determined by the way in which the metals interact with their environment. As an example, the electrical, magnetic and mechanical properties are the reaction of these materials to the electrical, magnetic and mechanical forces respectively. Other important properties are the thermal properties such as heat transfer and capacity, the optical properties such as scattering, absorption and transmission of light, and the chemical properties such as corrosion resistance. The study of materials science is very important for the establishment of materials with special nature to use it in special applications, where these new materials have low manufacturing cost and high performance. Like all other things, materials are grouped into groups to understand their nature, where one can

classify them basing on their properties, use or structure. New metal combinations (alloys) are very important in our life and we need it in many scientific and industrial fields:

- Engine performance is increasing at high temperatures, which require structural metals to resist this high temperature.
- Dealing with nuclear power or energy requires solving the problems of nuclear wastes which leads us to manufacture the nuclear wastes containers.
- Aircrafts that flying at supersonic speeds need to be manufactured from light and strong materials and have a great resistance to high temperatures levels.
- Optical communication lines require the manufacture of the optical fibers with very little absorption of light so that the absorption calculations can be neglected.
- Civil and military buildings are constructed with strong materials which have high resistance to corrosion.

The need for materials with high performance, strength and affordable cost has led to develop a new solidification process such as rapid solidification. The rapid solidification technology (RST) has a significant contribution to the alloy's increased solubility, reduction in segregation, and increased refinement of the material grain size. The combination of such factors adjusts the materials microstructure and mechanical properties, therefore, it is useful in managing the behavior of materials, especially those required in sensitive applications. This technique allows manufacturing alloys with higher yield strength and better microstructures [2].

In the present thesis the following steps have been accomplished:

1. The conventionally solidified (CS) Al-5Zn-2.5Mg alloy ingots have been prepared in a vacuum furnace.
2. The rapidly solidified (RS) ribbons have been produced using the melt-spinning technique with different wheel speeds of (10, 50, and 80) m/s and fixed temperature (850°C).

These CS samples and RS ribbons have been tested by Vickers Microhardness Tester (VMT) to calculate the diagonals of indentation. All specimens have been tested with a Universal Testing Instrument for the tensile testes. The CS and the MS samples have been characterized using the Scanning Electron Microscopy (SEM) which applies an electron beam instead of light, an electron detector in instead of eyes, and a screen



and camera to view the results. The X-Ray Diffraction (XRD) has been used to obtain the microstructures patterns. Finally, the Differential Thermal Analysis (DTA) has been applied for thermal analysis and the.

Following this introductory, chapter 2 contains general information about the materials used in this study and the necessary background information about the previous studies that have been done on the Al-Zn-Mg alloys. Chapter 3 contains some information about the devices that used to analyze the obtained alloys samples and the experimental methods of the present work. The chapter 4 contains the obtained results and their discussion. Finally, chapter 5 contains the thesis conclusion.

## **CHAPTER 2**

### **GENERAL INFORMATION**

Since the Al-Zn-Mg alloy is being investigated, general information should be given about the components, namely aluminum (Al), zinc (Zn), and magnesium (Mg).

#### **2.1. ALUMINUM**

Aluminum is a metal with silvery – white color mentioned in the periodic table as the thirteenth element [1] and has properties which made it one of the engineering materials keys in the latest decades. We can find aluminum in our homes, in the transportation machines we use such as cars, trains, aero planes, ships, etc. In the computers and mobile phones we use in a daily basis. But 200 years ago, very little information were available about this metal. An interesting fact about aluminum is that it is the most widespread metal in the composition of the planet, which is more than 8% of the nucleus mass of the Earth's core. It's also in the third place of the most popular chemical element on Earth after oxygen and silicon. Pure aluminum does not exist in nature separately because of its high ability to blend with other elements. This is the reason for its late knowledge by mankind. Officially, aluminum was produced in 1824 for the first time and it took 50 years to learn how to produce it industrially. The most widespread form of aluminum found in nature is aluminum sulphates which gives the aluminum, its name. Today we know more than 300 different types of aluminum and metal compounds that have a certain percentage of aluminum like feldspar, ruby, sapphire, and emerald, which are far less common. Despite it's widespread in nature, it would have remained unknown and undiscovered forever if electricity had not been detected. The scientists used electricity to separate the chemical compounds. In the 19th century, Danish physicist, Christian Orested, used the electrolysis to obtain the aluminum. Since then, the electrolysis has been used to extract aluminum, these days as well. Aluminum gives a remarkable combination of worthy properties as it is one of the lightest elements on Earth and is three times lighter than iron [2]. However, it has a strong, flexible and corrosion resistance structure due to being covered with a strong and thin layer of oxide film. Aluminum is non-magnetizable and is an excellent electrical conductor also it can

form many different alloys. Aluminum is an element that can be treated even at high or low pressures and temperatures. It can be pulled, stamped, and rolled. It is an element that does not ignite, does not require a special dye and is also nontoxic. It is also a very flexible element so that it can make a chip that does not exceed the thickness of little macrons from it. Furthermore, it is used to make extra thin foils which are less than three times the thickness of human hair [3]. Moreover, it is less expensive than many metals and materials. Since aluminum has the ability to easily form many different compounds with other materials, a wide range of alloys were produced and developed using aluminum. An aluminum alloy is a chemical compound that is produced by adding some materials to pure aluminum in order to develop and improve its properties, initially to enhance its strength [4]. Even by adding a small percentage of mixtures can radically alter the properties of the metal, making it suitable for use in new areas that were previously unusable. As an example of the diversity of aluminum compounds, we can find aluminum mixed with silicon and magnesium in the wheels and engines of the cars and in other parts of modern cars design. In the meantime, the scientists continued to manufacture and develop alloys, considering aluminum as a base element. Modern industries such as aviation, energy, vehicles, food industries and many other industries would not have existed without aluminum. Moreover, aluminum has become an icon of progress, this mixture of exceptional properties is what made aluminum on the top of the list of most desired elements and entangled in modern industries. In addition to these features, aluminum has another advantage no less than its predecessors, which is the advantage of recycling. Aluminum and its alloys have the ability to melt repeatedly and restructure without any damage or detriment to its mechanical properties. More than three-quarters of the amount of aluminum produced from the beginning of its discovery and so far, is present and currently used.

## **2.2. ZINC**

Zinc is a silvery-white metal which have a blue hue, and it has the ability to tarnish in air. The Romans have been known zinc but they rarely used it. The production of zinc in China in the form of large quantities was in 1500 AC, as a ship belonged to the east India company sank in 1745 off the coast of Sweden, which was carrying a zinc made in China, When the scientists analyzed the extracted packages, they concluded that the

Chinese had discovered a way to obtain almost pure zinc. Zinc is used to paint other metals, especially iron, for strength and corrosion resistance. Galvanized steel is used for cars structure, streets lamp poles, safety barriers in the highways and a lot of construction cases. The majority of the zinc amounts are used to produce die-casting, which is of great importance in the automotive industry, the electricity industry, and many other industries. It is also used in alloys like brass, nickel, silver, and aluminum solder [4]. The main locations for zinc mining are located in China, Australia, and Peru. At present, the international companies produce the equivalent of 11 million tons per year of zinc, which is used in the manufacture of many useful alloys.

### **2.3. MAGNESIUM**

Magnesium is a silver-white metal that has a flammable ignition and is ignited in the form of a glowing light. Magnesium exists in a way that is associated with other elements in nature. Although, it is the eighth most plentiful element in the Earth's crust, it is found in huge deposits in minerals such as dolomite and magnesite. Water bodies, like the oceans and seas, are the main source of magnesium production, with more than 850,000 tons per year being produced. Magnesium is produced by processing magnesite ( $\text{MgO}$ ) with silicon or by the electrolysis of dissolved magnesium chloride  $\text{MgCl}_2$ . It is one-third less dense than aluminum. When it is added to the aluminum as an alloying agent, it improves the fabrication, welding and mechanical characteristics of the aluminum. These alloys are useful in aero plane and car construction [5]. Magnesium is used to produce lightweight materials [6], such as car seats, laptops, luggage, power tools and cameras. It is also added to the molten iron and steel to remove sulfur. To gain the benefit from combustion when it is in contact with air, magnesium is widely used in the fireworks industry, sparklers and flares [7]. Magnesium oxide is used to fabricate heat-resistant bricks for furnaces and fireplaces. Magnesium sulfate is sometimes used as a caustic for dyes. Magnesium hydroxide is added to cattle feed and fertilizers. Magnesium components also used in medicine. It has been put in vehicles for the first time in pure magnesium frames, such as racing bicycles giving a better composition of lightness and strength than other metals, the structures made of magnesium are three times lighter than those made of steel. As a metal, magnesium is alloyed with a few percent of aluminum, plus crumbs of zinc and manganese, to enhance strength, corrosion resistance and welding qualities, also it is

used to economize energy by making things lighter to minimize fuel flow and gravity when moving. Magnesium can be recycled at very little expense in all these products [8].

## 2.4. ALLOYS

The simplest definition of impurities (alloys) is a metal consisting of at least two different chemical elements, the first is the main element and the other added to it by a certain percentage. The main element is usually 90% or more of the total volume. Other elements can be metals or non-metals added in smaller quantities to the alloy, comparing with the main metal. There are international standards on which aluminum alloys are classified and these are characterized by four figures numbers [9], the first figure corresponds to the main component of alloys. The second figure corresponds to the variations of the initial alloy. The third and fourth figures correspond to individual alloy variations.

**Table.1.** Aluminum alloys groups

<b>Alloy Group</b>	<b>Principal alloying element</b>
1xxx	Pure Al (99.00 % or greater)
2xxx	Copper
3xxx	Manganese
4xxx	Silicon
5xxx	Magnesium
6xxx	Magnesium and Silicon
7xxx	Zinc
8xxx	Other elements

### 2.4.1. THE IMPORTANCE OF ALLOYS

The humankind was forced to produce and use the alloys because of the inability of the original metals to carry out the tasks needed by humans, especially during the period of industrial revolution. Where the iron is a strong metal and useful in construction, but

steel is stronger, tougher and less susceptible to corrosion [10]. Also note that the aluminum is light metal but soft and tender in its original state. Adding a little magnesium, manganese and copper to pure aluminum will get a combination of these minerals, called duralumin, which is used in the aircraft industry because of its hardness and light weight. When producing alloys, they show qualities that exceed the qualities possessed by the main metal component. As a scientific fact, the alloys are more powerful, have less elasticity and are more resistant to the expansion of the main metals. Therefore, the purpose of producing alloys is to obtain new materials with more suitable properties for the new works assigned to them. Moreover, these properties are also controlled by the way these impurities are manufactured with. The crucial need for high durability, high effectiveness, and cost efficient materials have resulted in the use of modernistic processing mechanism to improve a new aluminum alloys for structural usage [11].

#### **2.4.2. THE IMPORTANCE OF THE Al-Zn-Mg ALLOYS**

The Al-Zn-Mg alloy is one of the aluminum alloys which have a good age-hardening capability and has the highest calculated hardness values among the other aluminum alloys. It is used in many different industrial applications because of its high hardness properties, light weight and strong resistance to corrosion. Thus, these alloys encouraged major interest in the aviation and transportation industry [12]. Zinc and magnesium are the primary alloying elements, high Zn: Mg attribution produces the best strength and reaction to heat treatment, side by side with the highest susceptibility to stress corrosion. Low ratios make the best weld capability and the lowest quench sensitivity. Al-Zn-Mg alloys used exceedingly in aerospace manufacture, promoted and powerful weapon systems and automobile industries according to their magnificent mechanical characteristics advanced by age hardening [13].

## 2.5. BACKGROUND

Many scientific works have been done during the previous decades concerning on the obtaining of the Al-Zn-Mg alloys. Many authors have noted the mechanical and microstructural changes that take place on these alloys. In the present study we will mention some of these scholarly works.

7012 alloys have been studied by Ferragut *et al.* [14] to investigate the microstructural evolution of this alloy during the first stages of the artificial ageing. The alloys compositions were Al-6Zn-2Mg-1Cu (wt%) with minority contents of Zr, Mn, and Ti, of 0.12, 0.10, and 0.06 (wt%) respectively. A disk shaped samples with certain dimensions of 1.5 mm thickness and 10 mm diameter for the positron lifetime measurements have been done, which were polished, cut and thermally treated. Supposing that the metastable phase  $\eta$  boundaries for these alloys is identical to those in the Al-Zn-Mg alloys, despite of the existence of Zr, Mn, Ti, or Cu the 150 °C temperature which used as an ageing temperature is higher than the metastable phase boundaries, the average volume and size of the fraction of particles observed in the 7012 alloys for different thermal treating has been recorded. The observed results for the average particle size: for 8 and 1 minute at 150 °C (artificial ageing),  $0.7 \pm 0.1$  nm and  $0.9 \pm 0.1$  nm respectively. For 5 days and 5.5 months as pre-ageing were the same reading ( $1.0 \pm 0.1$  nm). The results of the volume fraction of the observed particles were: for 8 minutes artificial ageing at 150 °C was  $1 \times 10^{-3}$ . For 5 days and 5.5 months as pre-ageing were the same reading ( $1-2 \times 10^{-3}$ ). The artificial ageing results showed that the primary influence of the heat treatment is a fast decrease of the microhardness and positron lifetime.

A HREM study by Li *et al.* [15] has been done on the 7108 alloys with composition of 92.94 Al-5.4 Zn-1.2 Mg-0.16 Zr (all in wt%) with a tiny amount of Cu, Mn, Si, and Fe to investigate the structure of the  $\eta$  phase which is very important for the age-hardening precipitates in the commercial alloys (Al-Zn-Mg). The study has been done at the atomic level by a source of high resolution electron microscopy (HREM). The solution has been treated at 480 °C and then quenched to room temperature followed by two stages artificial ageing heat treatment for 5 hours at 100 °C and for 6 hours at 150 °C. The samples have been grounded to thin foils after cut in to plate form. It has been

noticed that the electron diffraction spots for the  $\eta$  phase were very weak and wide spread comparing with those in the aluminum matrix. A few spots could experimentally observed even a huge amount of the  $\eta$  phase reciprocal lattice exists. The HREM tests were primarily executed along the [111] and [112] of the aluminum zone axes. It has been found that the generality of the  $\eta$  precipitates to be 3-4 nm along the c-axis, while in the a-b axes plane were 5-6 nm. It has been assured that the  $\eta$  phase has a hexagonal lattice with 0.496 nm on the a-axis and 1.402 nm on the c-axis, and the HREM images are providing useful structural properties of the age-hardening precipitates. Finally a comparison has been made between the obtained models and the models that mentioned in the previous studies in the same field, and a new model has been suggested on the basis of the structural properties that recorded in the HREM images.

Jiang *et al.* [16] investigated the influence of zirconium and copper on the early stages of aging in the Al-Zn-Mg alloys. The alloys combinations concentrations were Al-5.5 Zn-1.15Mg, Al-5.4Zn-1.24Mg-0.16Zr and Al-5.4Zn-1.22Mg-0.16Zr-0.29Cu. The study based on the fact that adding cooper to these alloys gives it an enhanced strength, also adding zirconium could lead to control grain size and recrystallization degree because adding cooper and zirconium to the mentioned alloys make an influence to the Guinier-Preston (GP) zones formation causing a huge impact on the formation of metastable transition phase leading to enhance the mechanical characteristics. It has been worked on two groups of samples for the investigated alloys obtained from different aging processes, the first group has been aged at room temperature for various times instantly after quenching. The second group has been pre-aged also at room temperature for 0, 7, and 28 days, followed by aging for 5 and 20 hours at 100 °C. The previous papers results [17-21] have been expressed which notified that the addition of zirconium to these alloys (Al-Zn-Mg) impedes and inhibits the formation of GP zones and the metastable phase, also it slows down the precipitations of the stable phase and restrains the nucleation of T phase (Al-Zn-Mg phase). While adding cooper to the ternary Al-Zn-Mg alloys enhances the nucleation of GP zones and expedite the nucleation of the metastable phase at lower temperatures and making the aging time shorter, subsequently expediting the aging reaction of the alloys. Moreover, adding copper to these ternary alloys increases the maximum temperature limit of GP zones formation and its stability, which may be a result of the change in GP zones composition.



Berg, *et al.* [22] investigated the texture of GP- zones using the TEM methods for Al 7108 alloys with primary alloying elements of 5.36 % Zn, 1.21 % Mg and 0.16 % Zr. The zirconium has been added to make a cube of  $\text{Al}_3\text{Zr}$  dispersoid and that led to form additional spots at the  $[1,0,0]_{\text{Al}}$  position and so on in the direction models. After the artificial ageing, the samples have been prepared for the TEM tests from various steps throughout the double ageing treatment, which expanded to the optimal hardness (T6) and over aged (T7). The specimens also have been studied after natural ageing. It has been observed that GPI zones are shaped over a vast range of temperature, from room temperature to 140 °C-150 °C independently of the quenching temperature. On the other hand, GPII zones were shaped after quenching from above of 450 °C, by ageing at above 70 °C.

The quantitative characterization of the precipitate free zones (PFZ) in the Al-Zn-Mg (-Ag) alloys have been investigated using the microchemical analysis and nanoindentation measurement by Ogura *et al.* [23]. The alloys compositions were Al-4.86Zn-1.78Mg- $<0.01$ (Ag, Cu, Mn, Cr, Si, and Fe), and Al-4.89Zn-1.78Mg-0.28Ag- $<0.01$  (Cu, Mn, Cr, Si, and Fe) all in (mass %). The nanoindentation measurement has been carried out around the grain borders, moreover, the micro Vickers hardness was measured and the observation and the EDX analysis have been performed. From the isothermal aging curves of hardness for the Al-Zn-Mg alloys which aged at 433K, it has been showed that the increase in hardness is clearer and the summit hardness of the Ag-added alloy is higher than that in the ternary alloys. The precipitates exist inside the grains were specified to be metastable state and or stable state from the symmetrical diffraction manners. The PFZ has been spotted straight along the grain borders with a width less than 500 nm. A clear observation couldn't be done for the change of the PFZ with the aging time, it has been attributed that to the difference of contact angles between contiguous grains. It has been observed that huge accounts of fine precipitates are disseminated homogeneously inside the grains. While a larger precipitates were created with smaller number of density in the PFZ neighborhood particularly in the samples under peak- and over- aged situation. Using the EDX analysis the variation in solute concentrations across the grain border has been examined to maintain the compositional information around it. Mg and Zn concentrations are both obtained at

scales of volume concentrations in the area far enough from the grain borders. Furthermore, it has been cleared that the concentrations of Mg and Zn were less in the PFZ and the area just outside the PFZ. It has been proposed that the solute atoms dislodged to the grain borders. According to the direct monitoring of nanoindentation marks, the hardness inside the PFZ has been obtained to be lower than those inside the grains. On the other hand, in the area just outside the PFZ, the hardness also decreases towards the grain borders.

Marlaud *et al.*[24] investigated the 7150 alloy of Al-6.4wt%Zn-2.3wt%Mg-2.2wt%Cu composition with addition of 0.08wt%Fe, 0.06wt%Si, and 0.12wt%Zr+Ti, and 7449 alloys of Al-8.5wt%Zn-2.2wt%Mg-1.9wt%Cu composition with addition of 0.08wt%Fe, 0.06wt%Si, and 0.13wt%Zr+Ti. It has been concentrated on the composition of precipitates in these alloys systems for various heat treatments. In order to differentiate between metallurgical states, anomalous X-ray small-angle scattering (ASAXS) has been used to describe the structure of precipitates quantitatively and measure incessantly the procedures on-going throughout the heat treatment. The atom probe tomography (APT) has been also applied to supply some of the missing information. After more, by using the TEM and DSC measurements, it has been obtained more basic descriptions of the studied alloys. The main results can be abbreviated as the following: It has been found that the precipitates contain exactly 33 at % Mg and 10-15 at % Al near to equilibrium condition, Cu content is about 13at% regardless of the alloy content. The precipitates contain almost zero Cu at 120 °C, and it is increasing gradually to 3-10 at% at higher temperatures of (135-160 °C). A huge variations in the remaining solid solution has been found at peak-aging, according to the surplus alloy ration between the content of Zn+Cu and Mg. Throughout the different treatment, it has been viewed the variety in the precipitate compositions in these alloys to be appropriate with a kinetic control because of the slow diffusion of Cu in Al comparing to Mg and Zn atoms. Also, it has been viewed that the composition of the precipitates can be adjusted by tuning the alloy composition and the heat temperature. Meanwhile, the quantity of the Al in the precipitates has no huge sensitive to these processed parameters, also the exchanging atoms between Zn and Cu can be partially controlled.

Yazdian *et al.* [25] worked on the microstructural evolution of nanostructure 7075 aluminum alloy during the isothermal annealing. Al-Zn-Mg and Cu as a powder have been used to create nanostructural Al 7075 alloy with composition of Al-5.6% Zn-2.5% Mg-0.6% Cu by the mechanical alloying technique which executed in high energy planetary ball mill for various milling periods. A super saturated solid solution has been obtained by using the ball milling method. The XRD test showed that the milling powders of (Al-5.6wt%Zn-2.5wt%Mg-1.6wt%Cu) have a noticeable decrease in their intensities due to the crystalline size refinement and lattice strain enhancement. It has been found that when the milling time is up to 15 hours, this will lead to disappear the Zn, Mg, and Cu peaks. On the other hand, the Al peak will shift to higher angles. It has been suggested that this may be because of the fractional decomposition of Zn, Mg, and Cu in the aluminum lattice and the grain boundaries. In the primary steps of the mechanical alloying method, it has been observed a sever microhardness increasing because of the solid solution hardening of the Zn, Mg, and Cu also due to the grain size refinement and MgZn precipitation phase. It has been confirmed that the type and stability of the intermetallic composition which precipitates in the matrix of aluminum are relay on the annealing time.

Deng *et al.* [26] investigated the influence of Mg content on the quench sensitivity of the Al-Zn-Mg-Cu aluminum alloys. The Al-8.0Zn-x Mg-1.6Cu alloys have been prepared in the laboratory using ingot metallurgical route. The purity of the natural materials was (99.998%) for all. Using an electrical resistance furnace, the metals have been melted in a crucible made of graphite. After pouring the liquid metal in an iron mold, the ingots has been left to be homogenized at 400 °C and 470 °C for 12 hours. The Hardness tests have been applied on the resultant alloys. The hardness tests showed that the  $H_v$  max increased by increasing the amount of Mg where when Mg = 1.0%, 1.4%, and 2.0%, the  $H_v$  max was 167, 173, and 197  $H_v$  respectively. This relation refers to that the prevalent strengthening particles of the Al-Zn-Mg-Cu alloy are metastable particles  $\eta$ , and raising the amount of Mg will increase the amount of the  $\eta$  phase particles leading to be clear that the Mg has a great influence on the quench sensitivity (higher Mg content  $\rightarrow$  higher sensitivity).

Premixed Al-5.6-6.4wt%Zn, 2.4-3wt%Mg, 1.5-2wt%Cu, 0.1-0.3wt% Sn have been

studied by Taleghany *et al.* [27] to investigate the microstructural and mechanical characterization by cold compaction and hot extrusion. The major ingredient of the premix was atomized pure aluminum powder mixed with master alloy powder consist of all the alloying components. After lubricating,  $\text{MgZn}_2$  has been showed as the main intermetallic phase which detected in the microstructure. Yet, the size of the  $\text{MgZn}_2$  phases and its morphology which showed in the microstructure of the lubricated compact and the pre sintered compact in the XRD patterns are somewhat different. It has been observed that the higher hardness of the as-water- quenched compacts demands higher loads of extrusion.

Using the TEM device, the precipitates structures in the Al-Zn-Mg alloys were observed with the addition of Cu/Ag by Watanabe *et al.* [28]. The concentrations that have been used were Al-6 mass%Zn-2 mass% Mg-0.3 mass% Si as a base alloy with addition of 0.49 mass%Cu and 0.74 mass%Ag. These alloys have been casted in a constant mold. Using the hot extrusion method, plates of 15 mm width and 1.5 mm thickness have been executed, after that rolled to plates of 1.0mm thickness. Heating and quenching have been applied, after that the heat treatment has been performed in oil bath at 423 K and 473 K. The maximum hardness for the base and the addition alloys has been recorded at 423 K as: base alloy 130  $H_v$ , Cu addition alloy 157  $H_v$ , and Ag addition alloy 159  $H_v$ . For 473 K as: base alloy, Cu addition alloy, and Ag addition alloy were 74  $H_v$ , 114  $H_v$ , and 128  $H_v$  respectively. Likewise, it has been showed that the addition of Ag and Cu present a higher hardness comparing with the base alloy. Furthermore, Cu and Ag addition alloys implicate a greater precipitate density comparing with the base alloy.

The Microstructure and mechanical properties of the Al-6Zn-2.5Mg-1.8Cu alloy prepared by squeeze casting and solid hot extrusion had been investigated by Fang *et al.* [29]. The alloy has been prepared under different specific pressures which started with increasing the pressure from 0 to 250 MPa. It has been noticed that the dendrites started to become round and small, it has been also noticed that the phases of  $\text{MgZn}$  decreases due to the pressure changes, but when the pressure reached 250 to 350 MPa, the grain size increased. After solid hot extrusion, the ultimate tensile strength was 605.67 MPa and the elongation was 8.1%, which were amended about 32.22% and 15.71% respectively, comparing with those of the metal mold casting alloy.

Acer *et al.* [30] studied the effect of the growth rate on the microstructure and microhardness in a directionally solidified Al-Zn-Mg Alloy. The Al-5.5wt%Zn-2.5wt%Mg ternary alloy has been produced by preparing it in a vacuum melting furnace and a casting furnace. The specimens were directionally solidified upwards at a fixed temperature gradient,  $G$  (5.5 K/mm), with various growth rates,  $V$  (8.3 to 165)  $\mu\text{m/s}$ . The primary dendrite arm spacing ( $\lambda_1$ ) has been measured by calculating the space between the nearest two dendrites tips using two methods of measuring. The first was the triangle method, where the triangle shaped by attaching the three adjacent dendrites centers and the side of the triangle corresponding to  $\lambda_{1(\text{tr})}$ . At least 50-200  $\lambda_1$  data were measured for every sample. The second method was the area counting method. By using linear regression analysis, the reliance of the dendritic spacing and microhardness on the growth rate has been determined. Finally, comparisons have been done among growth rate,  $V$ , microstructure, and Hall–Petch-type relationships, which have been obtained in the experiment, with those of former studies in the same field.

Acer *et al.* [31] also investigated the mechanical and microstructural properties of the Al-5.5wt%Zn-2.5wt%Mg alloy as-cast under heat-treated conditions. Alloys specimens have been homogenized under various statuses then aged under various systems to investigate the effect of heat treatment. By using the OM, SEM, and TEM, the effects of heat treatment on the microstructures has been studied, also the mechanical properties of the alloy have been studied. By successive and suitable heat treatments, good compositions of high microhardness and reasonable tensile strength have been obtained. It has been observed that the type of fracture varied significantly from ductile to more ductile relying on the aging system by using a Fractographic analysis of the tensile fracture surfaces.

While many works have been issued and studies have been done to investigate the Al-Zn-Mg alloys obtained by different compositions and methods, as far as we know, no studies dealt with these alloys in a compositions of Al-5Zn-2.5Mg obtained by the melt-spinning technique with different wheel speeds of (10, 50, and 80) m/s and fixed temperature of 850 °C. Therefore, the aim of this thesis is to investigate the mechanical and microstructural properties of the as-cast samples and the melt-spun ribbons for this

alloy. The alloy samples have been characterized using the Vickers microhardness tester (VMT) to calculate the diagonals of indentation. The specimens have been tested with universal testing instrument for tensile testes. The scanning electron microscopy (SEM) and the X-ray diffraction (XRD) have been applied to obtain the microstructures patterns. Finally, the differential thermal analysis (DTA) has been applied. The data have been collected, discussed and compared with the results of the conventionally solidified samples of the same alloy.

## CHAPTER 3

### MATERIALS AND METHODS

#### 3.1. MATERIALS

##### 3.1.1. MELT SPINNING TECHNIQUE

The Melt Spinning Process (Fig.3.1) is a technique used for rapid cooling [32] using a rotated hollow wheel generally cooled from inside by water or liquid nitrogen. By applying a gas pressure, the molten composition is then leaked on to the wheel surface, which rotates at a certain speed. When the metal fluid touches the wheel surface, it solidifies rapidly. This technique is used to improve materials that require high hardening speed in order to let metallic glasses be formed. The cooling rates executed by this technique are about  $10^4$ – $10^8$  Kelvins per second (K/s). The melt-spun alloys exhibit a unique microstructure, decreased segregation, very fine grain size, and potentially, enhanced its characteristics.

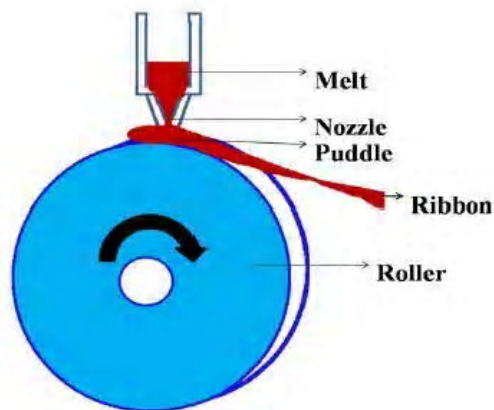


**Figure 3.1.** Melt spinning process [33].

### 3.1.2. VICKERS MICROHARDNESS TESTER (VMT)

The hardness is the resistance to indentation, and it is specified by measuring the constant depth of the indentation. VMT (Fig.3.2) can be used for testing the metals, ceramics, and composites microhardness testing, also it can test very thin materials like foils, measure individual microstructures in a huge matrix, or calculate the hardness gradients of a section over the cross section. The obtained indentation is calculated and transformed to hardness values [34].

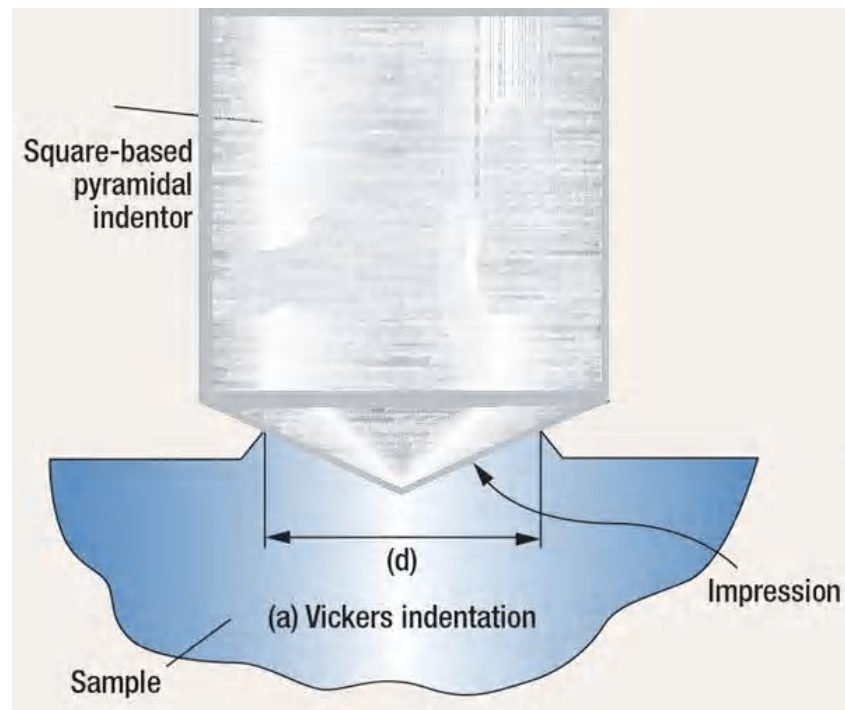


**Figure 3.2.** Vickers microhardness test [35].



### 3.1.3. UNIVERSAL TESTING MACHINES

Many kinds of testing machines exist but the most common type is the universal testing machine, which test different types of materials while they were under tension, compression or bending. Two classes of testing machines exist, electromechanical and hydraulic. The electromechanical devices use an electric motor, gear reduction system and 1, 2 or 4 screws to shift the crosshead up or down [36]. A zone of crosshead speeds will be able to be obtained by modulating the speed of the motor by the software control (Fig.3.3).

The main components of the universal testing machine are:

- Actuator
- Attachment kit
- Measuring and safety devices

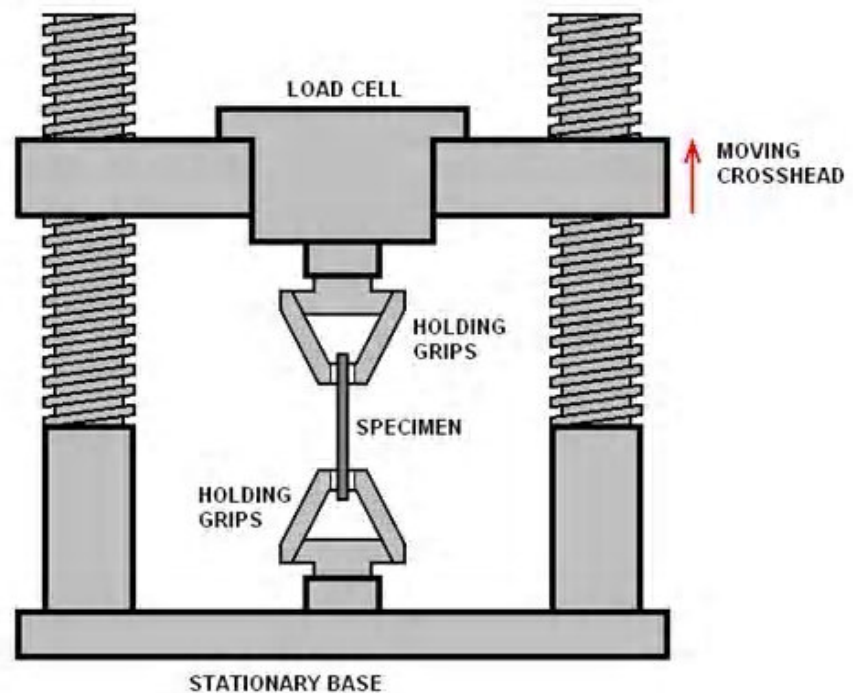


**Figure 3.3.** Tensile Strain test schematic [37].

### 3.1.4. SCANNING ELECTRON MICROSCOPE (SEM)

The SEM is a powerful microscope (Fig.3.4), it uses electrons instead of light to view objects in great details. The shorter wave of electron permits useful magnifications about 100.000 times versus about 2000 times for light microscopy it also provide much greater depth of field than light microscopes allowing complex three dimensional objects to remain sharp and in focus [38].

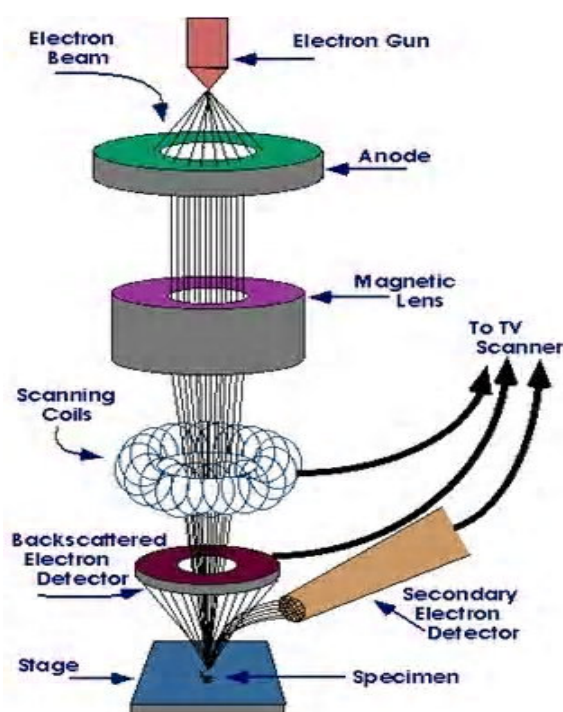


**Figure 3.4.** SEM analysis schematic [39].

### 3.1.5. X-Ray DIFFRACTION (XRD)

The XRD is a powerful technique for materials analysis which illustrates the information about structure and content of the physical and essential properties of the specimen [40] (Fig.3.5). It is useful to record the average spacing between layers of the atoms, finding the crystal structure for the materials, determining the orientation of a single crystal or grain, and to measure the size, internal stress and the shape of small crystalline regions.

The XRD is working with Bragg's law ( $n\lambda = 2d\sin\theta$ ) where:

$\lambda$  = the wave length of the rays.

$\theta$  = the angle between incident rays and the surface of the crystal.

$d$  = spacing between layers of atoms

The constructive interference occurs when  $n$  is an integer so the reflected waves for different layers perfectly in phase with each other and maintain a bright point, otherwise it will be either missing or unreal.

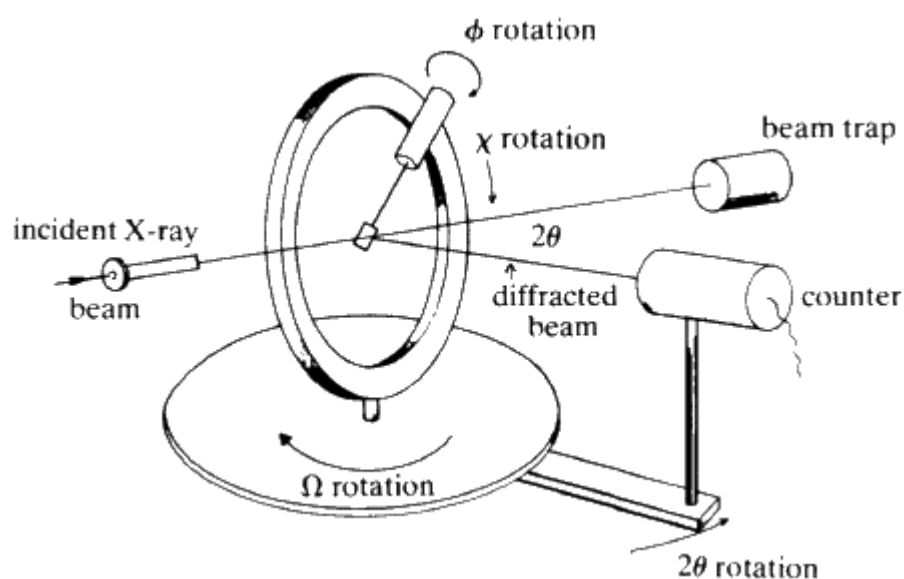


**Figure 3.5.** XRD analysis principle [41].

### 3.1.6. DIFFERENTIAL THERMAL ANALYSIS (DTA)

The DTA is a process in which the difference between the sample and thermally inert reference substance temperatures is repeatedly calculated as a function of temperature /time. This process produces values of a considerably more fundamental nature. The thermogram consists of a record of the difference between specimen and reference temperature and plotted as a function of the furnace temperature [42]. If there is a zero temperature difference between sample and reference material, the sample does not undergo any chemical or physical change, but if any reaction takes place, the temperature difference ( $\Delta T$ ) will occur between the sample and reference material (Fig.3.6).

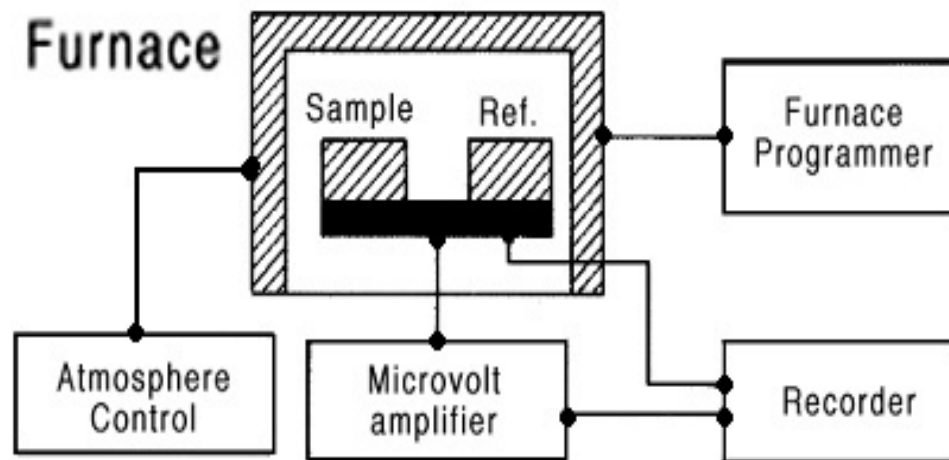


**Figure 3.6** DTA schematic [39].

### 3.2 EXPERIMENTAL METHODS

A conventionally solidified (CS) alloy ingot samples with nominal composition of Al-5Zn-2.5Mg have been produced in a vacuum furnace by casting 99.99% pure aluminum, 99.99% pure zinc and 99.99% pure magnesium (Fig.3.2). Using the Meta cut device (Fig.3.3) the ingot has been cut in to small parts (Fig. 3.4).



**Figure 3.2.** The CS alloy ingot.



**Figure 3.3.** Metacut-m250 device [44].



**Figure 3.4.** Sectioned samples.

alloy has been placed and re-melted in a Graphite crucible (Fig.3.5) which attached to the melt-spinning device.



**Figure 3.5.** Graphite crucible.

Using an induction coil with temperature of 850 °C applied on the alloy composition then by subjecting a pressure of argon in to the molten alloy inside the crucible, a stream of this molten alloy has been ejected through a 0.5 mm diameter orifice on to the brass wheel of the melt-spinning device (Fig.3.6) leading to create the melt-spun (MS) ribbons (Fig.3.7).

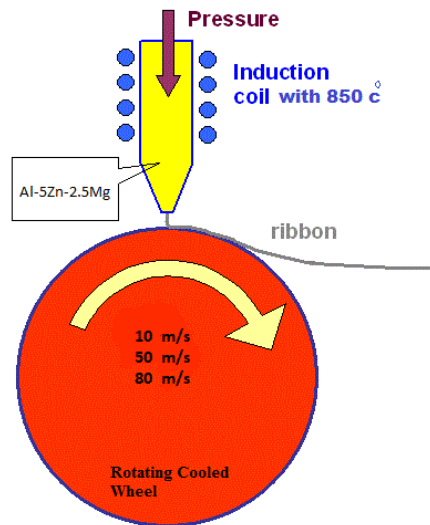


**Figure 3.6.** Melt-spinning process.

**Figure 3.7.** MS alloy ribbons.

The ejected samples of the alloy have been solidified using different wheel speeds of 10, 50, and 80 m/s. Furthermore, by using Struers Labopress1 device (Fig.3.13) with adding hot mounting-process clips (Fig.3.8) and mounting resin (granules), the hot mounting samples (Fig.3.9) have been produced. The MS ribbons samples have been cut in to 2.5 cm long and placed in the elevate bar of the Struers Labopress1 device (it should be cleaned and powdered to prevent samples from sticking). This 2.5cm MS ribbons samples have been adjusted using the hot mounting-process clips, then pouring the hot mounting resin granules of 2.25cm<sup>3</sup> for the MS ribbons samples and 1.5cm<sup>3</sup> for the CS sectioned ingot samples.



**Figure 3.7.** Struers Lapopress 1 device





**Figure 3.8.** Hot mounting process clips



**Figure 3.9.** Hot mounting ribbon sample

The hot mounting ribbons samples and sectioned ingot samples were created by adjusting the device at 180°C and 20 Kn for 5 minutes then 3 minutes cooling using water stream.

For polishing the surface of the hot mounted MS ribbons samples and sectioned CS ingot samples, Struers Labopol 5 (Fig.3.10) has been used, which is a grinding and polishing machine with 1200 and 1500 grit.



**Figure 3.10.** Struers Labopol 5 device [45]

After polishing for few minutes a diamond suspension (Fig.3.11) has been poured to obtain extra smooth surface.



**Figure 3.11.** Diamond Suspension

The MS ribbons samples and sectioned CS samples have been separated and kept in transparent plastic bags and the name of the sample has been written on the bags (Fig.3.12). For the CS samples and the MS ribbons hardness calculations, HVDM3 model digital microhardness device has been used at room temperature. The Vickers indenter with different loads of 0.098, 0.245, 0.49, 0.98, 1.47, and 1.96 N has been used for 10s as a loading time to calculate the diagonal of indentation with  $\pm 0.1\mu\text{m}$  accuracy. The average of ten measured data at various locations of the samples surface has been taken for each sample. A pre designed device (AG-10KNG) Shimadzu universal testing has been used to execute the uni-axial tensile test at room temperature and testing the stress-strain responses of all the CS samples and the MS ribbons alloys. Two seals had been stuck on the specimens instead of the conventional clip gauge, and by observing the distance between those two seals using a video camera the strains measurement has been started, with the help of a computer contains data acquisition software to collect the data.

The scanning electron microscopy (SEM) has been carried out using the FEI Quanta 250 FEG device for inspecting topographies of the specimens at very high magnifications. Throughout the SEM examination, an electrons beam is focused on a spot volume of the sample, making the energy transfers of to the spot.





**Figure 3.12.** The MS ribbons and CS samples after hot mounting and polishing

These bombarding electrons eject electrons from the samples itself. The ejected electrons, are collected by a positively biased detector, and then transformed into a signal. Furthermore, the XRD diffractometer has been used to determine the phase structure of the conventionally solidified and the melt-spun ribbons alloys. The diffraction with adjusted values of 160 mA, 40kV and 10°/min has been executed using Cu K $\alpha$  radiation filtered by graphite. Using the DTA device with 10 °C/min in argon protection at temperature range of 30-1000 °C, a thermal analysis has been applied on these samples.

## CHAPTER 4

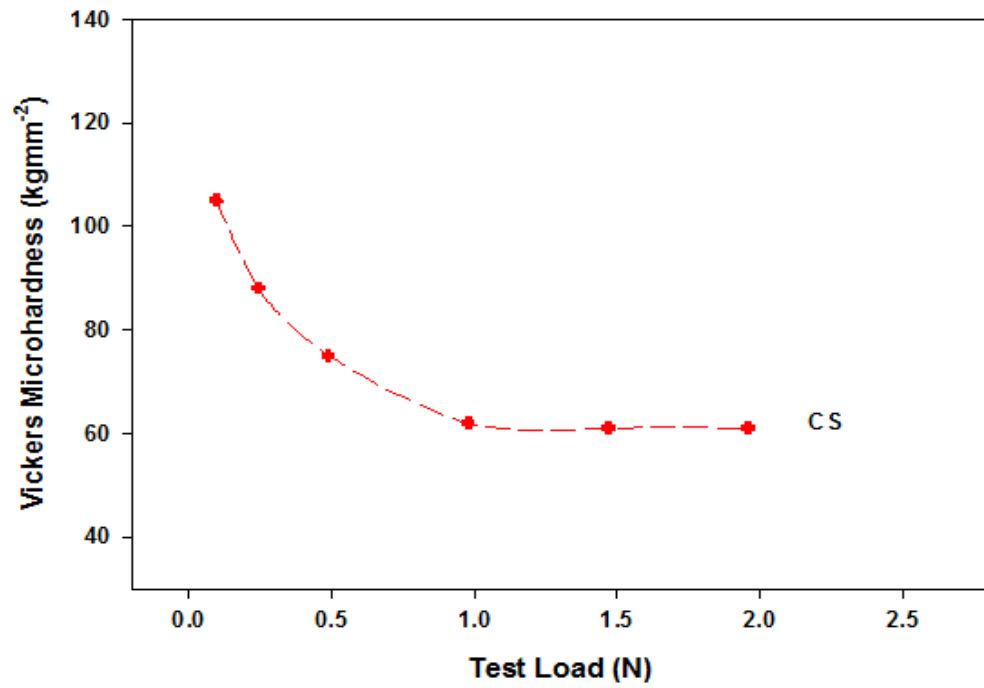
### RESULTS AND DISCUSSION

#### 4.1 THE MECHANICAL PROPERTIES

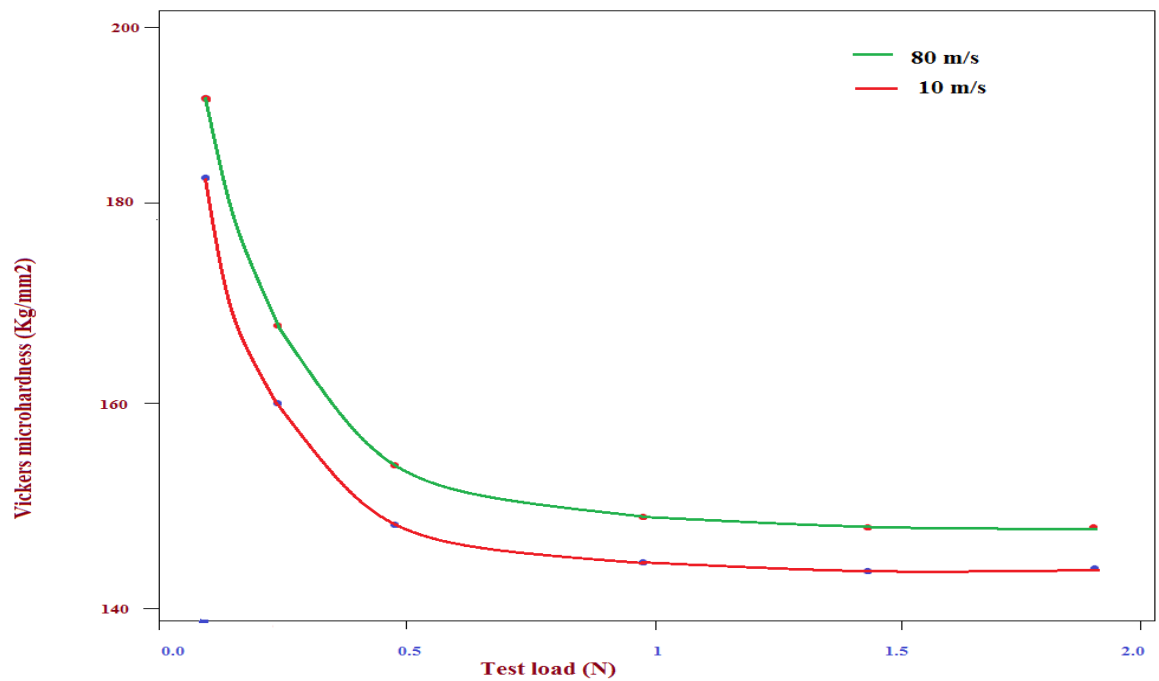
The mechanical properties of any solidified material are usually determined with the hardness test, tensile strength test, ductility test, etc. Since true tensile strength testing of solidified alloys gave inconsistency results with a wide scatter due to their strong dependence on solidified sample surface quality, the mechanical properties were monitored by hardness testing, which is one of the easiest and most straightforward techniques [46]. In this study, the mechanical properties of the conventionally cast samples and their rapidly solidified ribbons were determined by Vickers microhardness measurements. The reported hardness  $H_v$  calculated according to the equation [11]:

$$H_v = \frac{2P \sin(\theta/2)}{d^2} = \frac{1.8544(P)}{d^2}$$

Where P is the indentation force, d is the average diagonal length and 1.8544 is a geometrical factor for the diamond pyramid. As performed in the previous literature studies [47-49] the tests have been started with (0.098 N) to measure the Vickers hardness value ( $H_v$ ) of the CS samples and the melt-spun specimens. Fig.4.1 shows the variation of the Vickers microhardness values with the applied test loads of the CS alloy's samples. Fig.4.2 illustrates the variation of Vickers microhardness values ( $\text{Kgmm}^{-2}$ ) with the applied test loads (N) for the melt-spun Al-5Zn-2.5Mg alloy ribbons with wheel speeds of 10 and 80 m/s. It is obvious that the ribbons solidified with maximum wheel speed (high cooling rate) have the higher microhardness values for the same applied test load comparing with that in the CS samples and in the minimum wheel speed MS ribbons. The Vickers tests did not applied on the MS ribbons for the 50 m/s wheel speed in order to make a comparative between the minimum and maximum wheel speeds.



**Figure 4.1.** The variation of the Vickers microhardness values with applied test load for the CS samples.



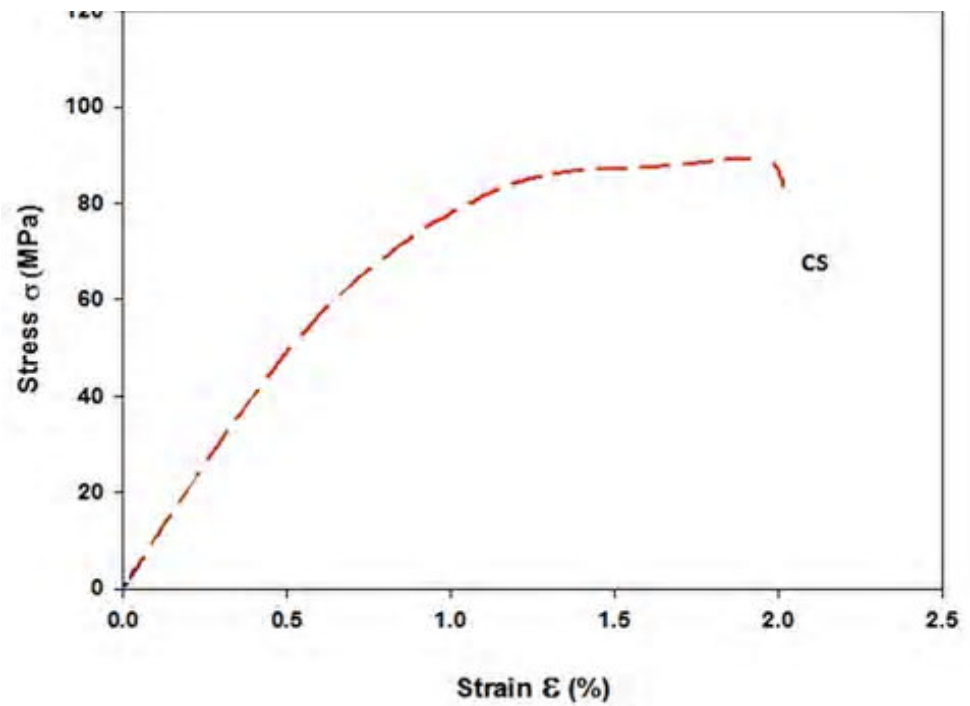
**Figure 4.2.** The variation of the Vickers microhardness values with applied test load for the MS ribbons of 10 and 80 m/s.

Table 2 shows the applied test loads and the corresponding microhardness values for the melt-spun Al-5Zn-2.5Mg ribbons for the minimum and maximum wheel speeds. It can be concluded that when the solidification has a higher cooling rate (wheel speed) the degree of nanocrystalline phase increases so does the hardness.

**Table 2.** The Dependence of the microhardness ( $H_v$ ) on wheel speed of 10 and 80 m/s for the melt-spun Al-5Zn-2.5Mg ribbons and the CS samples.

Test load (N)	CS Sample $H_v$ (Kgmm <sup>-2</sup> )	10m/s $H_v$ (Kgmm <sup>-2</sup> )	80m/s $H_v$ (Kgmm <sup>-2</sup> )
0.098	105	183	192
0.245	88	160	169
0.49	75	150	156
0.98	62	145	150
1.47	61	144	149
1.96	61	144	149

Another aim of this study was to compare the tensile stress ( $\sigma$ ) values of the conventionally cast and the melt-spun Al-5Zn-2.5Mg alloy. Typical stress-strain curve from tensile test in the conventionally cast samples is shown in Fig. 4.3. It can be observed that the conventionally cast samples had a highest tensile stress value in 90 Mpa until the rupture point occurred and elongation about 2%. On the other hand, the tensile stress curves of Al-5Zn-2.5Mg ribbons obtained by wheel speeds of 10 and 80 m/s shown in Fig.4.4, where as seen from this figure, the highest tensile stress until the rupture point occurred and elongation values of the ribbons with wheel speed of 10 m/s was 180 Mpa and 0.9% respectively. While the highest tensile stress until the rupture point occurred and elongation for ribbons with wheel speed of 80 m/s were 190 Mpa and 0.9% respectively. The rapidly solidified ribbons show superior mechanical properties comparing with the conventionally cast counterparts which are attributed to the precipitates of intermetallic compound in the Al matrix and refinement the microstructures.



**Figure 4.3.** Engineering stress-strain curves obtained by the tensile tests at room temperature for the CS samples.

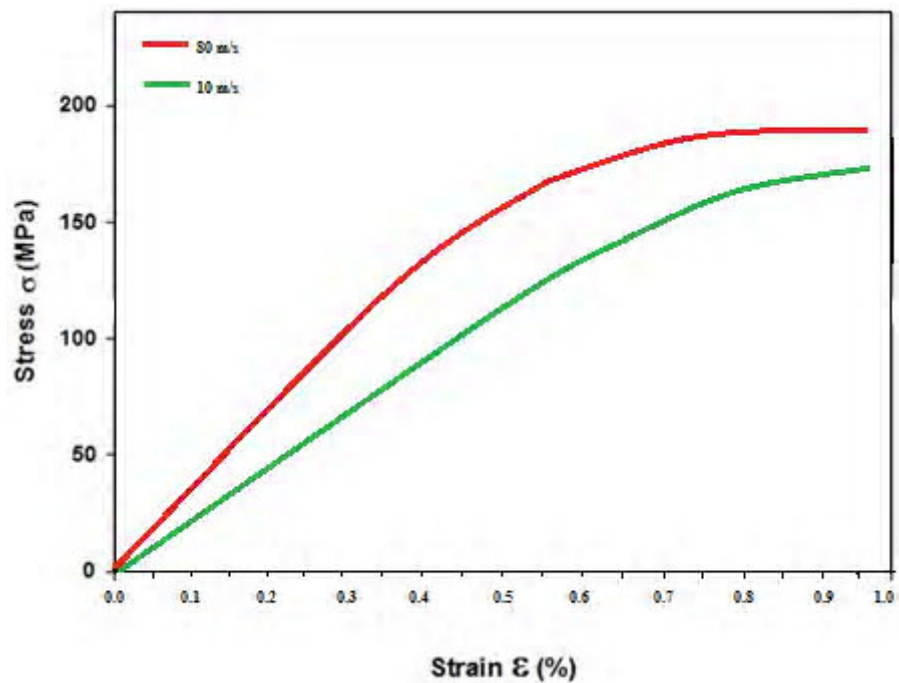


**Figure 4.4.** Engineering stress-strain curves obtained by the tensile tests at room temperature for the melt-spun ribbons with wheel speeds of 10 and 80 m/s.

## 4.2. THE SEM MICROGRAPHS

In order to obtain the microstructural characterization, the conventionally solidified ingot samples have been studied by the SEM device. The as cast microstructures contain both dendritic  $\alpha$ -Al solid solution and non-equilibrium phases which are the intermetallics that mainly precipitate on the grain boundaries and interdendritic space during solidification. Therefore, during solidification, the distribution of the  $\alpha$ -Al solid solution and the intermetallics are uneven and composition segregation usually occurs too as shown in Fig. 4.5 which reveals the intermetallic constitutions of  $\text{Al}_{12}\text{Mg}_{17}$  and  $\text{MgZn}_2$  in the  $\alpha$ -Al matrix for the CS samples after exposing to the SEM device. In addition, uneven distribution of cooling rates, temperature, impurity, chemical element, metallic or non-metallic inclusion, and so on can also result in inhomogeneous phenomenon [50].

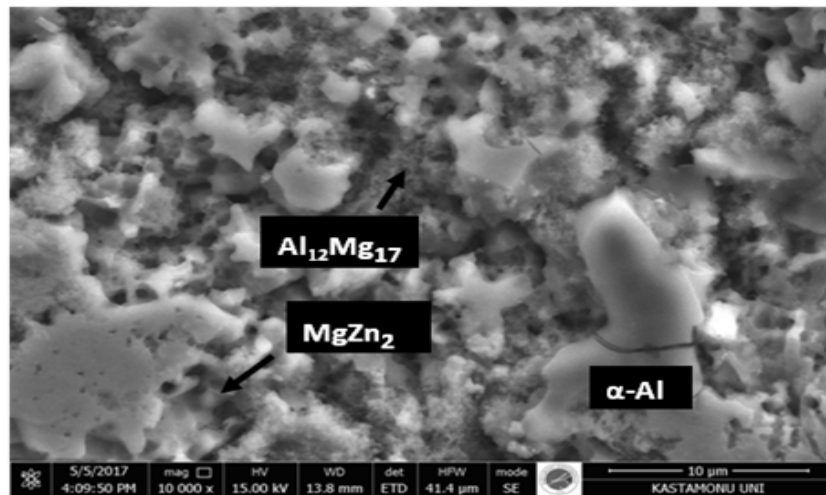


**Figure 4.5.** The SEM images for the CS sample.

The MS ribbons were also studied by the SEM photographs. After applying the samples to the rapid solidification process, it can be seen that the melt-spinning technique can make changes to the phase constitution and apply a significant effect on the Al based intermetallics. This fact has been also seen in Ref. [51] where the melt-spun alloy with composition of Al-8Si-1Sb has been investigated. Fig. 4.6 illustrates the melt-spun ribbons that rapidly solidified for wheel speed of 10 m/s, where it showed discontinues microstructure in which the intermettallic phases started to disappear in the  $\alpha$ -Al matrix.

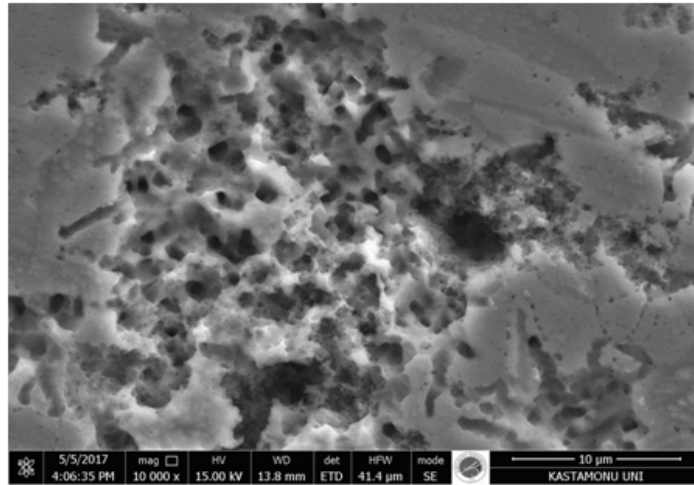


**Figure 4.6.** The SEM images for the MS samples at 10 m/s.

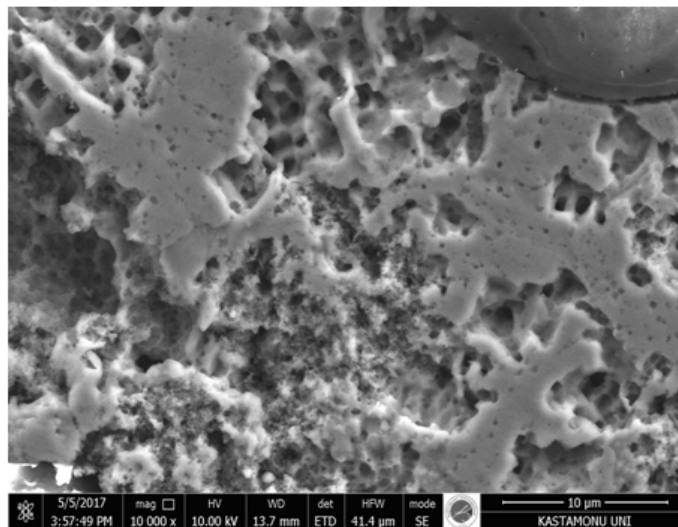


**Figure 4.7.** The SEM images for the MS samples at 50 m/s.

For the MS ribbons which rapidly solidified at wheel speeds of 50 and 80 m/s illustrated in Fig. 4.7 and 4.8 it can be seen that there are more homogenous distribution than that in Fig. 4.5 and 4.6. The morphology of the intermetallics is also influence by the solidification rates [52]. A higher solidification rate leads to smaller grain size and increases the particle numbers. This indicates that the high solidification rate of the melt-spinning process effectively improves the alloys composition homogeneity [53].





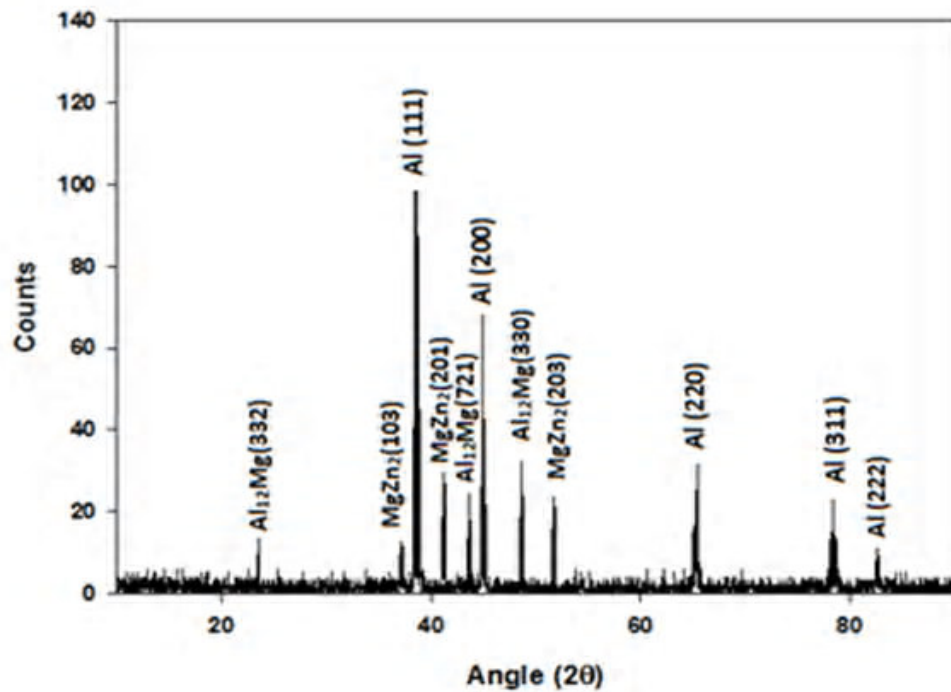


**Figure 4.9.** The XRD patterns for the CS samples.

Fig .4.10 illustrates the MS Al-5Zn-2.5Mg ribbons, for the minimum wheel speed of 10 m/s. It can be seen that there are three phases, two low intensity intermetallic phases namely  $\text{Al}_{12}\text{Mg}_{17}$  and  $\text{MgZn}_2$  and the  $\alpha$ -Al phase. The low intensity intermetallic peaks elucidate that there is some undissolved Zn and Mg which still exist in the aluminum matrix [55]. In Fig. 4.11 for 50 m/s wheel speed and Fig. 4.12 for the wheel speed of 80 m/s, it can be noticed that only the diffraction peaks of the Al solid solution are distinguished in the XRD pattern.

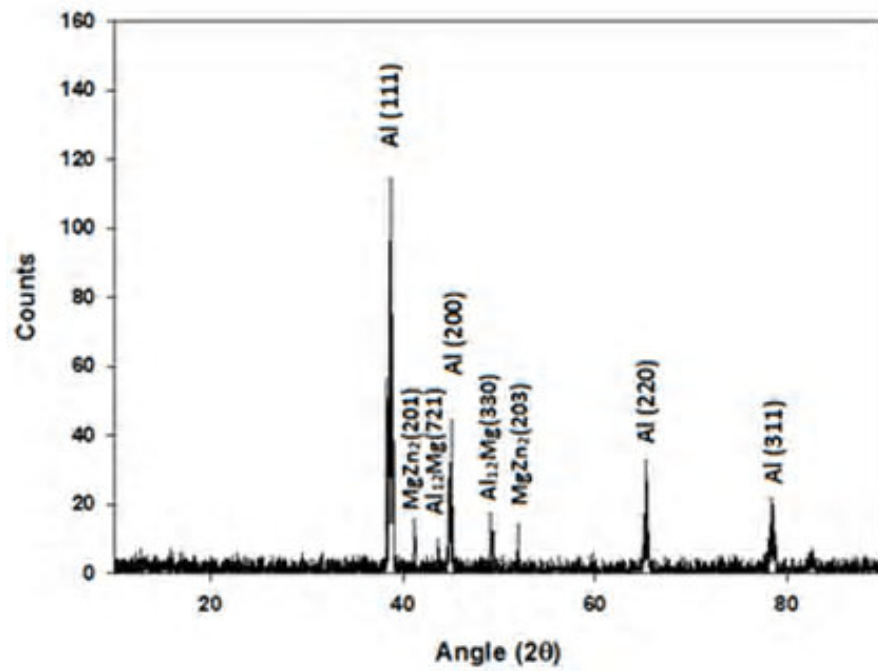


**Figure 4.10.** The XRD patterns for the MS samples at 10 m/s.

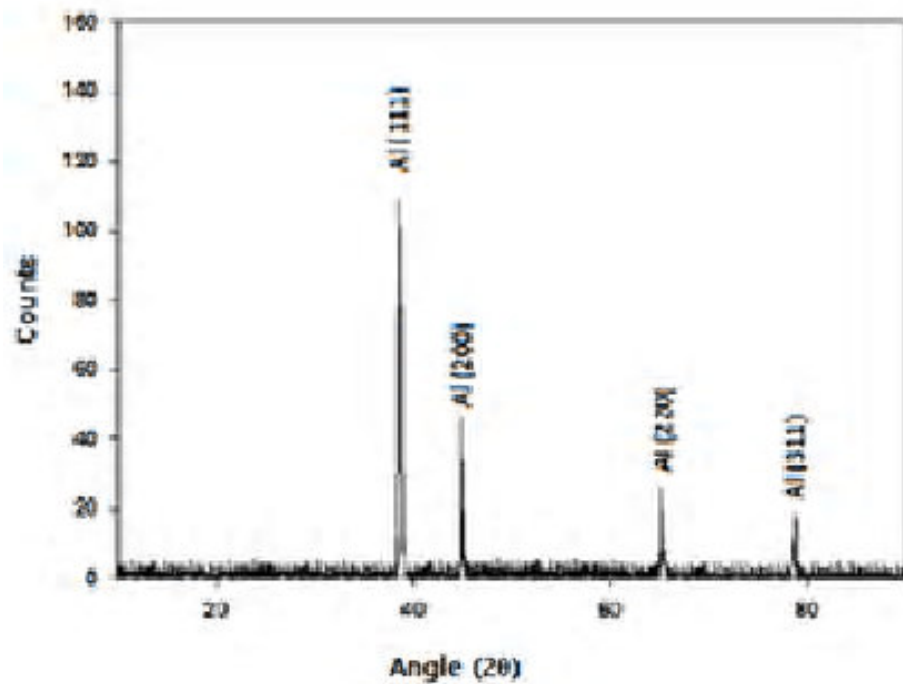


**Figure 4.11.** The XRD patterns for the MS samples at 50 m/s.

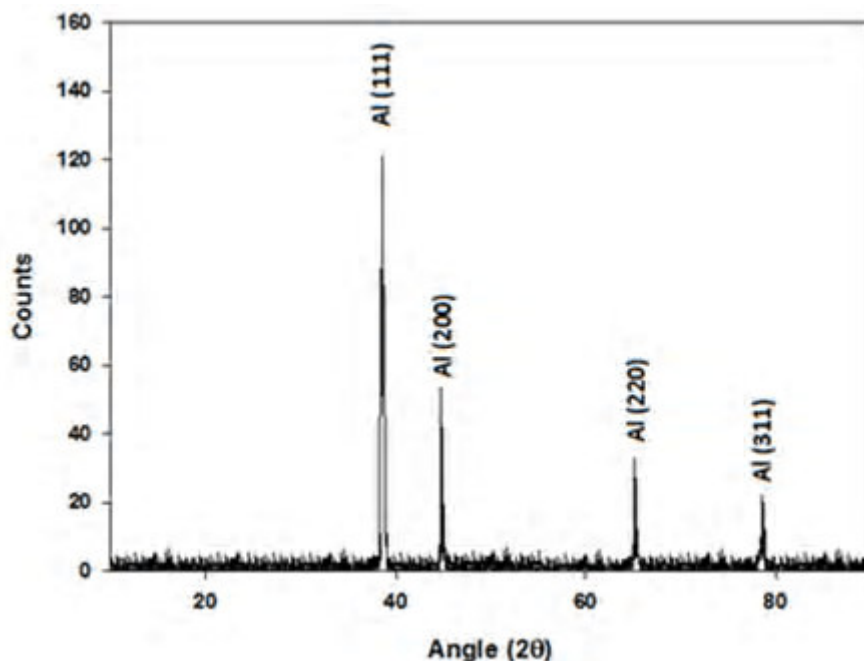


**Figure 4.12.** The XRD patterns for the MS samples at 80 m/s.

The melt-spinning technique has an effect on the alloys phase constitution, this can be seen in the Fig. 4.11 and Fig. 4.12 where the constitution of Zn and Mg in the Al matrix changed the phase structure of ingot alloys after the melt-spinning took place. As mentioned above, in the melt-spun alloys,  $\text{Al}_{12}\text{Mg}_{17}$  or  $\text{MgZn}_2$  were not detected in the XRD patterns for wheel speeds of 50 m/s and 80 m/s, that is probably because the amounts of the intermetallic phases are so small that they were undetectable by the XRD with a comparatively fast scanning rate of ( $10^\circ/\text{min}$ ). A part from the XRD limitation in detecting low volume concentrations, the absence of the intermetallic phases in the XRD pattern also revealed the extended solid solubility of the matrix after applying the melt-spinning method.

#### 4.4 THE DTA ANALYSIS

In order to examine the thermal stability of the melt-spun alloys, the DTA analysis has been applied. It is cleared that sharp peaks were observed for the melt-spun alloys. As can be seen in Fig. 4.13, the melting temperature of the Al-5Zn-2.5Mg melt-spun alloys obtained by wheel speed of 10 m/s was detected to be  $660^\circ\text{C}$  and the peak height to be  $44.72 \mu\text{V}$ , while in Fig. 4.14, the melting point of the Al-5Zn-2.5Mg melt-spun alloys

obtained by wheel speed of 50 m/s was observed to be 660°C and the peak height to be 33.62  $\mu\text{V}$ .

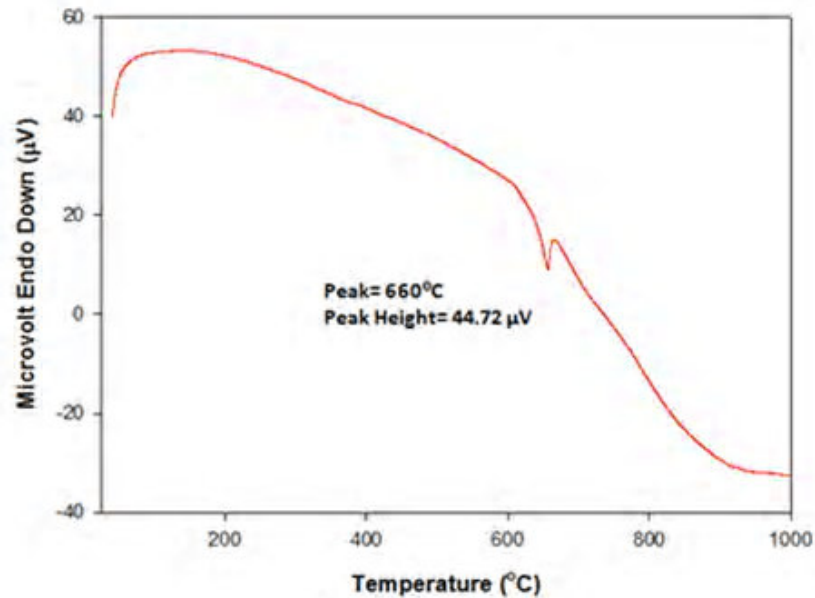


**Figure 4.13.** The DTA analysis for the MS samples at 10 m/s

Fig. 4.15 illustrates that the melting point of the Al-5Zn-2.5Mg melt-spun alloys obtained by wheel speed of 80 m/s was observed to be 662°C and the peak height to be 29.36  $\mu\text{V}$ . the wheel speeds affect the peaks more than the melting points, and if the wheel speed is too high, for example 80 m/s, the melting point increases very little.

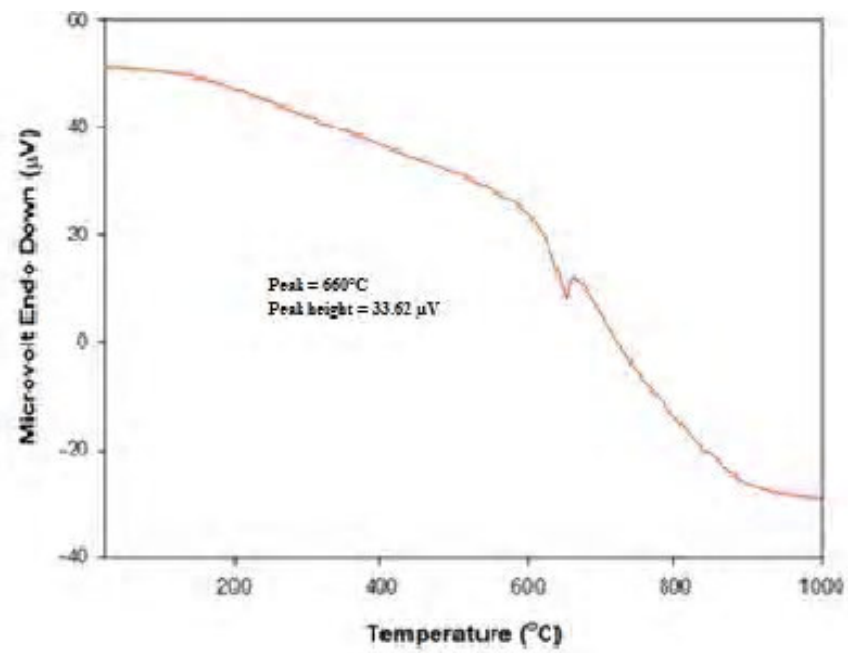


**Figure 4.14.** The DTA analysis for the MS samples at 50 m/s

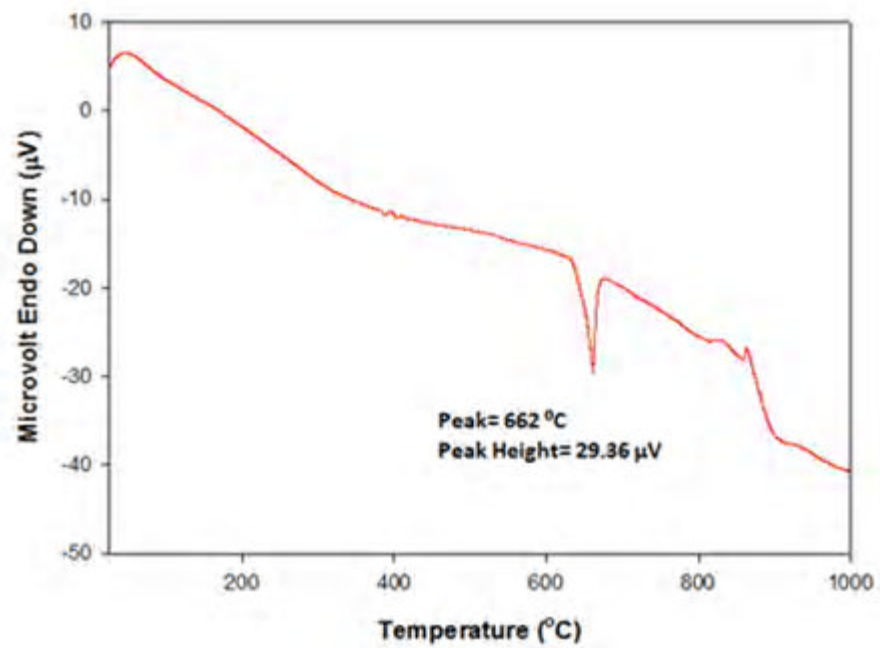


**Figure 4.15.** The DTA analysis for the MS samples at 80 m/s

We also studied the influence of the wheel speeds on the ribbon thickness and we found that the ribbons thicknesses was inversely proportional to the melt-spinning wheel speeds, in fact this is not the only factor that effect on the ribbon thickness, where the orifice diameter of the crucible, the temperature of the molten alloy, and the distance between the rotating wheel surface and the orifice of the crucible have also a great effect on the ribbons thickness [56]. Fig. 4.16 shows the relation between the melt-spinning wheel speeds and the ribbons thickness, whereas the wheel speeds increase the melt-spun ribbons thickness decreases.

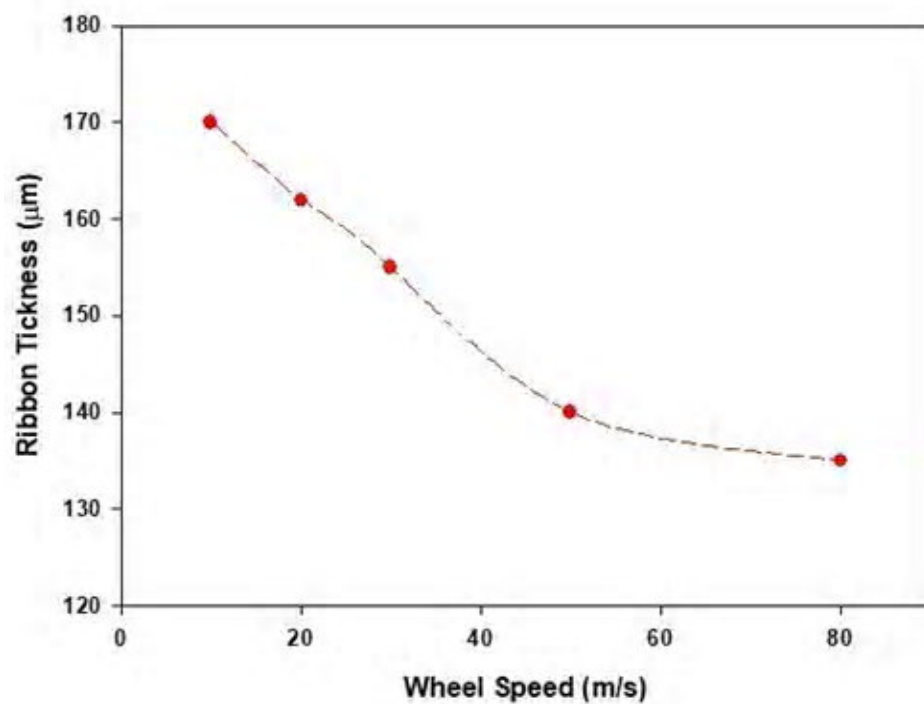


**Figure 4.16.** Variation of the ribbon thicknesses as a function of the wheel speeds for the Al-5Zn-2.5Mg MS samples.

## **CHAPTER 5**

### **CONCLUSION**

The present work investigated the structural and mechanical properties of the conventionally cast and the melt-spun ribbons for the Al-5Zn-2.5Mg alloy. These samples have been exposed to the SEM, XRD, DTA, Vickers tests and tensile stress tests where the conclusions can be summarized as following:

#### **5.1 The Vickers and Tensile Stress Results**

The micro hardness values for the Al based Al-5Zn-2.5Mg rapidly solidified alloy ribbons have been detected and it was obvious that there is an increasing in these values with the increasing of the melt-spinning wheel speeds. Also stress-strain tests have been applied on the conventionally solidified samples and the melt-spun ribbons. Comparing Fig. 4.3 with Fig. 4.4 it can be noticed that there are huge increase in the tensile stress ( $\sigma$ ) values, where the conventionally cast sample had a highest tensile stress value of 90 Mpa and elongation about 2% and the highest tensile stress and elongation for ribbons with wheel speed of 10 m/s was 180 Mpa and 0.9% respectively and the highest tensile stress and elongation for ribbons with wheel speed of 80 m/s was 190 Mpa and 0.9% respectively.

#### **5.2 The SEM Results**

The SEM Micrographs have been applied in order to obtain the microstructural characterization for the conventionally solidified and the melt-spun ribbons for the Al-5Zn-2.5Mg alloy samples. The conventionally solidified samples had dendritic  $\alpha$ -Al solid solution and non-equilibrium phases as shown in Fig. 4.5 the distribution of  $\alpha$ -Al solid solution and the intermetallics are uneven, this inequality in distribution can lead to inhomogeneous phenomenon. Rapid solidification has a great influence on the Al based intermetallics where it can change the phase constitution. Discontinuous microstructure in Fig. 4.6 shows that the intermetallic phases start to disappear in the  $\alpha$ -

Al matrix. For the melt-spun ribbons with wheel speeds of 50 and 80 m/s, it can be observed in Fig. 4.7 and Fig. 4.8 that there are more homogeneity than that in Fig. 4.5 and Fig. 4.6, that because of the higher solidification rate which cause a smaller grain size and higher particles number. The SEM analysis revealed that there are higher grains density and better homogeneity in the wheel side surface because of the higher solidification rate at the wheel side than that in the air side, while the air side has roughness and less homogeneity as shown in Fig. 4.8.

### 5.3 The X-Ray Diffraction Results

The XRD patterns for conventionally solidified Al-5Zn-2.5Mg sample revealed peaks related to three phases namely intermetallic phases ( $\text{Al}_{12}\text{Mg}_{17}$  and  $\text{MgZn}_2$ ) and  $\alpha$ -Al phase (Fig 4.9). The XRD results for the MS ribbons of 10 m/s wheel speed also showed the same three phases but with low intensity for the intermetallic phases in Fig. 4.10. On the other hand, it has been noticed that there are no peaks corresponding to the intermetallic phases for the melt-spun ribbons obtained with wheel speeds of 50 m/s and 80 m/s as seen in Fig. 4.11 and Fig. 4.12. The solidification rate was high enough to hold most of the alloying elements (Zn and Mg) in the Al matrix as a solid solution. In addition, it was obvious that the rapid solidification had a great effect on the phase constitution.

### 5.4 The DTA Results

The MS ribbons have been exposed to the DTA analysis to obtain the thermal stability. It has been noticed that the melting temperature of the Al-5Zn-2.5Mg ribbons with wheel speed of 10 m/s was 660 °C and the peak height of 44.72  $\mu\text{v}$ . For the MS ribbons of 50 m/s wheel speed the melting point was 660 °C and the peak height to be 33.62  $\mu\text{v}$ . While for the MS ribbons with wheel speed of 80 m/s the melting point was 662°C and the peak height was 29.36  $\mu\text{v}$ . The wheel speeds affect the peaks more than the melting points, and if the wheel speed is too high, for example 80 m/s, the melting point increases very little. An inverse proportional relationship has been obtained between the ribbon thickness and the melt-spun wheel speeds.



## REFERENCES

1. Stanley, C., 1968. Matter versus materials: A historical view. **Science**, **162**:637-644.
2. Gheiratmand, T., Hosseini, H.R., Davami, P., Ostadhossein, F., Song, M., Gjoka, M., 2013. On the effect of cooling rate during melt-spinning of FINEMET ribbons. **Nanoscale**, **16**:7520-7527.
3. Abobaker, M., Bouaziz, O., Lebyodkin, M., Lebedkina, T., and Shashkov, I.V., 2015. Avalanche dynamics in crumpled aluminum thin foils. **Scripta Materialia**, **99**:17–20.
4. Davis, J.R., 1998. Aluminum and Aluminum Alloys. **ASM International**, 351–416.
5. Frassinetti, S., Bronzetti, G., Caltavuturo, L., 2006. The Role of Zinc in Life: A Review. **Journal of Environmental Pathology, Toxicology, and Oncology**, **25** (3):597-610.
6. Afify, N., Gaber, A., Abbady, G., 2011. Fine Scale Precipitates in Al-Mg-Zn Alloys after Various Aging Temperatures. **Materials Sciences and Applications**, **2**:427-434.
7. De Baaij, J. H. F., Hoenderop, J. G. J., Bindels, R. J. M., 2015. Magnesium in Man: Implications for Health and Disease. **Physiol Rev.**, **95**:1–46.
8. Riegels, N., Michael, J. Richards, M. J., 2011. Humphry Davy: His life, works, and contribution to anesthesiology. **Anesthesiology**, **114**: 1282-1288.
9. Fernandes, A.I.M.T., 2011. Corrosion evaluation of Bare and Anodized Magnesium Alloys in Physiological Media. Technical University of Lisbon, Higher technical institute, Master thesis, Lisbon, 86 s.
10. Paleocrassas A. G., 2005. Feasibility investigation of laser welding aluminum alloy 7075-T6 through the use of a 300 w, single-mode, Ytterbium fiber optic laser. North Carolina State University, Graduate Faculty, Master thesis, Carolina, 89 s.
11. Musfirah, A.H, Jaharah, A.G., 2012. Magnesium and Aluminum Alloys in Automotive Industry. **Journal of Applied Sciences Research**, **8** (9): 4865-4875.
12. Karaköse, E., Keskin, M., 2011. Structural investigations of mechanical properties of Al based rapidly solidified alloys. **Materials and Design** **32**: 4970-4979.
13. Hunsicker, H. Y., 1976. Development of Al-Zn-Mg-Cu Alloys for Aircraft. **Mathematical and Physical Sciences** **282** (1307): 359-376.

14. Ferragut, R., Somoza, A., and Tolley, A., 1999. Microstructural evolution of the 7012 alloy during the early stages of artificial aging. **Acta Materialia**, **47**(17): 4355–4364.
15. LI, X.Z., Hansen, V., Gjønnes, J., and Wallenberg, L.R., 1999. HREM Study and structure modeling of the eta-prim phase, the hardening precipitates in commercial Al-Zn-Mg alloys. **Acta Materialia**, **47** (9): 2651-2659.
16. Jiang, X.J., Noble, B., Hansen, V., Taftø, J., 2001. Influence of Zirconium and copper on the early stages of aging in Al-Zn-Mg alloys. **Metallurgical and Materials Transactions A**, **32**: 1063-1073.
17. Mukhopadhyay, A.K., Shiflet, G.J., and Starke, E.A., Jr., 1990. Role of vacancies on the precipitation processes in Zr modified aluminum based alloys. **Scripta Metallurgica Materialia**, **24**:307-312.
18. Smith, W.F. Grant, N.J., 1970. The effect of two-step aging on the quench sensitivity of an Al-5Zn-2Mg alloy with and without 0.1Cr. **Metallurgical Transactions**, **1**:1735–740.
19. Garcia-Cordovilla, C. Louis, E., 1991. A differential scanning calorimetry investigation of the effects of zinc and copper on solid state reactions in Al-Zn-Mg-Cu alloys. **Materials Science and Engineering**, **A132**: 135-41.
20. Livak, R.J. and Papazian, J.M., 1984. Effect of copper on precipitation and quench sensitivity of Al-Zn-Mg alloys. **Scripta Metallurgica**, **18**: 483-488.
21. Park, J.K. Ardell, A.J., 1989. Correlation between Microstructure and Calorimetric Behavior of Aluminum Alloy 7075 and Al-Zn-Mg Alloys in Various Tempers. **Materials Science and Engineering**, **A114**: 197-203.
22. Berg, L.K., Gjønnes, J., Hansen, V., Li, X.Z., Knutson-Wedel, M., Waterloo, G., Schryvers, D., Wallenberg, L.R., 2001. GP-Zones in Al-Zn-Mg alloys and their role in artificial aging. **Acta Materialia**, **49**:3443–3451.
23. Ogura, T., Hirosawa, S., Sato, T., 2004. Quantitative characterization of precipitate free zones in Al-Zn-Mg (-Ag) alloys by microchemical analysis and nanoindentation measurement. **Science and Technology of Advanced Materials**, **5**: 491–496.
24. Marlaud, T., Deschamps, A., Bley, F., Lefebvre, W., Baroux, B., 2010. Influence of alloy composition and heat treatment on precipitate composition in Al-Zn-Mg-Cu alloys. **Acta Materialia**, **58**:248–260.

25. Yazdian, N., Karimzadeh, F., and Tavoosi, M., 2010. Microstructural evolution of nanostructure 7075 Aluminum alloy during isothermal annealing. **Journal of Alloys and Compounds**, **493**:137–141.
26. Deng, Y., Wan, Li, Zhang, Y., Zhang, X., 2011. Influence of Mg content on quench sensitivity of Al-Zn-Mg-Cu Aluminum alloys. **Journal of Alloys and Compounds**, **509**: 4636–4642.
27. Taleghani, J., Navas, R., Torralba, J. M., 2014. Microstructural and mechanical characterization of 7075 aluminum alloy consolidated from a premixed powder by cold compaction and hot extrusion. **Materials & Design**, **55**:674-682.
28. Watanabe, K., Matsuda, K., Ikeno, S., Yoshida, T., Murakami, S., 2015. TEM observation of precipitate structures in Al-Zn-Mg alloys with additions of Cu/Ag. **Archives of metallurgy and materials**, **60** (2):244-246.
29. Fang, H., LI, R., Chen, R., Yu, B., Qu, Y., Xun, S., Li, R., 2015. Microstructure and mechanical properties of Al-6Zn-2.5Mg-1.8Cu alloy prepared by squeeze casting and solid hot extrusion. **Trans. Nonferrous Met. Soc.**, **25**:2130-2136.
30. Acer, E., Cadirli, E., Erol, H., and Gunduz, M., 2016. Effect of Growth Rate on the Microstructure and Microhardness in a Directionally Solidified Al-Zn-Mg Alloy. **Metallurgical and Materials Transactions**, **47A**:3040-3051.
31. Acer, E. , Çadırlı , E. ,Erol, H., Kırındı, T., Gündüz, M., 2016. Effect of heat treatment on the microstructures and mechanical properties of Al-5.5Zn-2.5Mg alloy. **Materials Science & Engineering**, **A662**:144–156.
32. Budhani, R.C., Goil, T.C., and Chopra, K.L., 1982. Melt spinning technique for preparation of metallic glasses. **Bull. Mater. Sci.**, **4**(5): 549-561.
33. Nair, B., Priyadarshini, B.G., 2016. Process, structure, property and applications of metallic glasses. **AIMS Materials Science**, **3**(3): 1022-1053.
34. Coelho, B.N., Guarda, A., Faria, G.L., and Menotti, D., 2015. Automatic Vickers Microhardness Measurement based on Image Analysis. **Int'l Conf. IP, Comp. Vision, and Pattern Recognition, Athens** 249-255.
35. Mathers, G., 2017. Hardness testing part 1. ( Web page:<http://www.twi-global.com/technical-knowledge/job-knowledge/hardness-testing-part-1-074/>) (Date accessed: Oct. 2017).

36. Huerta, E., Corona, J.E., and Oliva, A.I., 2010. Universal testing machine for mechanical properties of thin materials. **Revista Mexicana De Fisica**, **56** (4):317–322.
37. Chaudhari, K., 2016. Tensile test. (Web page: <http://www.engineersgallery.com/tensile-test/>) (Date accessed: Oct. 2017).
38. Bogner, A., Jouneau, P.H., Thollet, G., Basset, D., Gauthier, C., 2007. A history of scanning electron microscopy developments: Towards “wet-STEM” imaging. **Micron**, **38**: 390–401.
39. Maurya, S., Sajeevan, S., warang, A., Paunikar, A., 2015. Automotive fasteners: defects and failure analysis. Department of automobile engineering, MES Pillai Institute of Information Technology, Engineering, Media Studies & Research. Bachelor thesis, Mumbai, 78 s.
40. Bunaciu, A., Udriștioiu, E.G., and Aboul-Enein, H.Y., 2015. X-Ray Diffraction: Instrumentation and Applications. **Analytical Chemistry**, **45**(4):289-299.
41. Clark, C.M., Dutrow, B.L, 2004. Single – crystal X- Ray Diffraction. (Web page: <https://serc.carleton.edu/details/images/8400.html>)(date accessed: Oct. 2017)
42. Jacob, S, 2011. Differential thermal analysis (DTA). ( Web page: <https://www.slideshare.net/shaisejacob/differential-thermal-analysis-dta-ppt>) (Date accessed: Oct. 2017).
43. Suresh, S., 2015. Analytical chemistry (differential thermal analysis) (Web page: <https://www.slideshare.net/sureshselvaraj108/differential-thermal-analysis>) (Date accessed: Oct 2017).
44. Metkon, 2013. Metacut series. (Web page: [http://www.metkon.com/en/category\\_metacut-series\\_47.html](http://www.metkon.com/en/category_metacut-series_47.html)) (Date accessed: Oct. 2017).
45. NYU Tandon School of engineering (Web page: <https://engineering.nyu.edu/composites/facilities/characterization>.) (Date accessed: Oct. 2017).
46. Ajao, J.A. 2009. Effect of Solidification Process Parameters on the Microstructure of Some Melt-spun Nickel-Based Hard facing Alloys. **Journal of Minerals & Materials Characterization & Engineering**, **8** (10): 775-785.

47. Karakose E, Keskin M. Morphological characteristic of the conventional and Melt-spun Al-10Ni-5.6Cu (in wt.%) alloy. **Materials Characterization**, **60**: 1569–1577.
48. Sahoo, K.L., Wollgarten, M., Haug, J., Banhart, J., 2005. Effect of La on the crystallization behavior of amorphous Al<sub>94</sub>-XNi<sub>6</sub>LaX (x = 4–7) alloys. **Acta Materialia**, **53** (14): 3861-3870.
49. Kaya, H., Cadırlı, E., Boyuk, U., Maraslı, N., 2008. Variation of micro indentation hardness with solidification and microstructure parameters in the Al based alloys. **Applied Surface Science**, **255**: 3071–3078.
50. Wang, H., Xu, J., Kang, Y., Tang, M., Zhang, Z., 2014. Study on inhomogeneous characteristics and optimize homogenization treatment parameter for large size DC ingots of Al–Zn–Mg–Cu alloys. **J. Alloy Compd.**, **585**:19–24.
51. Karakose, E. and Keskin, M., 2009. Effect of solidification rates on the microstructure and microhardness of a melt-spun Al–8Si–1Sb alloy. **J. Alloys Compd.**, **479**:230–236.
52. Kostyryhev, A.G., Slater, C.D., Marenych, O.O., and Davis, C.L., 2016. Effect of solidification rate on microstructure evolution in dual phase micro alloyed steel. **Scientific Reports**, 1-7.
53. Rafiei, A., Varahram, N., Davami, P., 2013. Microstructural study of Al-20Si-5Fe alloys produced by melt-spinning process. **Metall. Mater. Eng.**, **19** (1): 85-94
54. Solomon, I., Solomon, N., 2009. Melt-spun Fe-Co-Cr-B-Si alloys corrosion characterization. **U.P.B. Sci. Bull.**, **71**(4): 1454-2331.
55. Unlu, N., Genc, A., Ovecoglu, M.L., Eruslu, N., Froes, F.H., 2001. Characterization investigations of melt-spun ternary. **J. Alloys Compd.** **322**: 249– 256.
56. Hammood, A.S. and Jassim, A.K., 2014. Forming Technology to Produce Very Thin 5052 Al alloy Ribbons by Direct Casting from Liquid State. **International Journal of Mechanical & Mechatronics Engineering**, **14** (2): 128-131.

## **CURRICULUM VITAE**

**Name and surname:** Ali M. IBRAHIM

**Nationality:** IRAQ

**Birth date and place:** Baghdad 28/ 09/ 1972

**Marital status:** Married

**Cell phone:** 05340666065

**E-mail:** ali.mawlood@yahoo.com

**Correspondence Address:**

### **EDUCATION**

<b>Degree</b>	<b>Institution</b>	<b>Date of graduation</b>
M.Sc.	Erciyes University	2017
License	Mustansiria University	1996
High school	The Central High School	1990

### **FOREIGN LANGUAGE**

English